batteries

MDPI

Review

A Review of Lithium-Ion Battery Capacity Estimation Methods for Onboard Battery Management Systems: Recent Progress and Perspectives

Jichang Peng [1], Jinhao Meng [2,*], Dan Chen [2], Haitao Liu [1], Sipeng Hao [1], Xin Sui [3] and Xinghao Du [2]

[1] Smart Grid Research Institute, Nanjing Institute of Technology, Nanjing 211167, China
[2] College of Electrical Engineering, Sichuan University, Chengdu 610065, China
[3] Department of Energy Technology, Aalborg University, 9220 Aalborg, Denmark
* Correspondence: scmjh2008@163.com

Abstract: With the widespread use of Lithium-ion (Li-ion) batteries in Electric Vehicles (EVs), Hybrid EVs and Renewable Energy Systems (RESs), much attention has been given to Battery Management System (BMSs). By monitoring the terminal voltage, current and temperature, BMS can evaluate the status of the Li-ion batteries and manage the operation of cells in a battery pack, which is fundamental for the high efficiency operation of EVs and smart grids. Battery capacity estimation is one of the key functions in the BMS, and battery capacity indicates the maximum storage capability of a battery which is essential for the battery State-of-Charge (SOC) estimation and lifespan management. This paper mainly focusses on a review of capacity estimation methods for BMS in EVs and RES and provides practical and feasible advice for capacity estimation with onboard BMSs. In this work, the mechanisms of Li-ion batteries capacity degradation are analyzed first, and then the recent processes for capacity estimation in BMSs are reviewed, including the direct measurement method, analysis-based method, SOC-based method and data-driven method. After a comprehensive review and comparison, the future prospective of onboard capacity estimation is also discussed. This paper aims to help design and choose a suitable capacity estimation method for BMS application, which can benefit the lifespan management of Li-ion batteries in EVs and RESs.

Keywords: lithium-ion battery; battery management system; capacity estimation; electric vehicle; battery degradation

Citation: Peng, J.; Meng, J.; Chen, D.; Liu, H.; Hao, S.; Sui, X.; Du, X. A Review of Lithium-Ion Battery Capacity Estimation Methods for Onboard Battery Management Systems: Recent Progress and Perspectives. *Batteries* **2022**, *8*, 229. https://doi.org/10.3390/batteries8110229

Academic Editor: Pascal Venet

Received: 7 October 2022
Accepted: 5 November 2022
Published: 9 November 2022

1. Introduction

On the background of energy crisis and global warming, applications such as renewable energy systems and new energy vehicles (Electric Vehicles (EVs) and Hybrid EVs) have become a necessary way of saving energy and decreasing carbon emission [1,2]. As the key component in the power supply of the EVs and Renewable Energy Systems(RESs) [3–5], the energy management of the battery pack directly affects its performance in various operation conditions [6,7]. Due to its high energy density, long service life, no memory effect, etc. [8,9], the Lithium-ion (Li-ion) battery has become a first choice for EVs and RESs [10]. For example, lithium iron phosphate (LFP) has a 90~140 Wh/kg energy density and up to 2000 life cycles, which usually consists of $LiFePO_4$ cathode and graphite anode. In addition, Li-ion battery chemistries also include lithium Nickel Manganese Cobalt oxide (NMC) and lithium Nickel Cobalt Aluminum oxide (NCA) with a higher energy density (140~250 Wh/kg) [11]. Recently, battery manufacturers have also developed new products with relatively superior performance, such as the blade battery (LFP) from BYD which has good thermal safety characteristics through nail penetration tests [12]. Thanks to its excellent properties, the scope of Li-ion batteries has also expanded to various areas like robots, Automated Guided Vehicles (AGVs) and consumer electronics. Especially, with the concept of low carbon, Li-ion batteries will play an important role in the future. According

to Research and Markets research data in Statista [13], the global lithium-ion battery scales to about 185 GWh in 2020, and the market is expected to grow to 950 GWh in 2026 as shown in Figure 1.

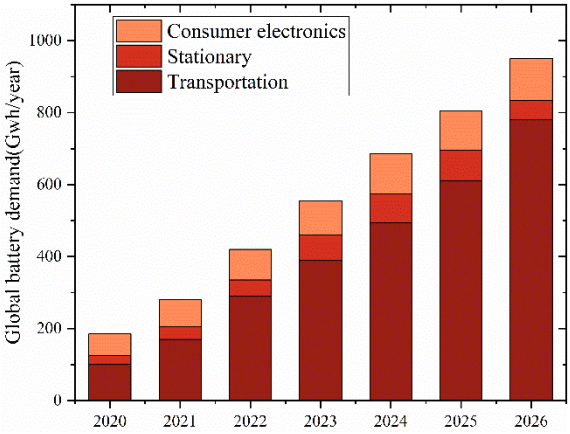

Figure 1. Global battery demand 2020–2026.

A typical structure of the Battery Energy Storage System (BESS) is illustrated in Figure 2, which mainly includes battery cells, Battery Management System (BMS), Power Conversion System (PCS), etc. Among all the components, BMS is responsible for the safety operation of the cells in the BESS. The functions of BMS include state estimation, voltage/temperature monitoring and fault diagnosis and warning. One key parameter here is the battery capacity representing the maximum Ah throughput at present. In essence, the battery capacity is the number and energy of the electrons inside the electrodes [14,15]. One consensus is that the Li-ion battery capacity will fade with battery degradation, which could be influenced by numerous external factors in operation conditions. Although the degradation of Li-ion battery can be briefly divided into two modes: Loss of Active Materials in electrodes (LAM), and Loss of Lithium Inventory (LLI), it is difficult to distinguish the aging modes in reality. However, the capacity of an Li-ion battery is critical for the energy management decision marking of BMS. For example, the battery State of Charge (SOC) represents current energy left, which is a ratio of the present Ah amount to its capacity [16]. It is impossible to obtain an accurate SOC without knowing the battery capacity. Once a precise SOC is received, BMS can choose when to charge or discharge each cell. In order to avoid the overuse of the Li-ion battery, its capacity should also be clearly defined. Otherwise, safety hazards, such as failure and thermal runaway [17,18], may exist when the Li-ion battery reaches its End-Of-Life (EOL) [19]. Capacity is also a fundamental index for the secondary use of the Li-ion battery [20,21]. In general, the battery capacity is especially important for the lifespan management of the cells by BMS [22,23].

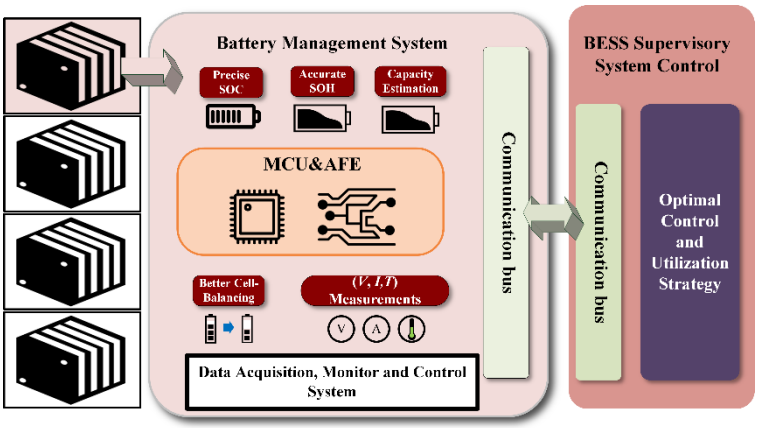

Figure 2. Structure of the battery energy storage system.

Battery capacity is usually regarded as the indicator of its lifespan, and it is believed to reach its EOL once the battery capacity reaches 80% of its initial value [24]. An accurate capacity can improve the accuracy of SOC estimation, thus enabling the users to perform charging operations and battery maintenance prompt. A slightly changed capacity will gradual deteriorate the battery's electrical and thermal characteristics and further lead to other severe safety issues [25]. However, a series of barriers hinder an accurately measurement of the Li-ion battery's capacity. One primary fact is the capacity of Li-ion battery is related to current rate and temperature [26,27] considering the effect of electrode kinetics. Then, it is easy to understand that the Li-ion battery's capacity greatly influences the working conditions of the battery pack, which increase the difficulties of obtaining an accurate battery capacity. Another critical factor is the limitation from BMS, the computing power of the microprocessor is limited due to the cost [28]. It can be deduced that onboard implementable battery capacity estimation algorithms are still needed for most EV applications [29,30]. One expectation is that the fast development of Internet-of-Things (IoT) and artificial intelligence can improve the capacity estimation techniques for BMS [31,32].

Great efforts have been made to obtain an accurate battery capacity in the literature, as shown in Figure 3. The points shown in the graph are the phrases that appear more than 20 times. The results of the high-frequency word analysis show a strong correlation between the battery capacity and the EVs. After analyzing the results, battery capacity is often used as an additional result for SOC estimation, or as a representation of energy and working efficiency. With the current market expansion and safety requirements, the battery capacity has become extremely important for battery health. From the analysis rules that brighter the node color means a more recent research period, the study of battery capacity has totally become a hot area with the keywords related to battery health all existing in brighter color. In the past, most works related to BMS focused on battery SOC [33,34]. With the wide application of EVs and RESs, the battery State-Of-Health (SOH), capacity, safety and Remaining Useful Life (RUL) are becoming the points of discussion. We have to mention that more than 500 articles have been investigated from 2016 to 2021; all related to battery capacity.

However, we also realized that there is a limited number of reviews on capacity estimation, especially for online implementable capacity estimation in BMS. Ref. [35] covers almost all the battery states including SOH, SOC, State-Of-Power (SOP), State-Of-Energy (SOE), etc., and selects the current research hotspots for discussion and evaluation. It is oriented towards the BMS and summaries the features of various states, but the capacity estimation methods are not well addressed. Refs. [30,36] provide a discussion of the classification of existing capacity estimation methods. Although the principles for the classification are different, they both discuss, in detail, the research methods, but [36] is more focused on the model-based method for Li-ion battery SOH estimation, and [30] published in 2015 has not covered any discussions about machine learning based methods. Most of the existing reviews on battery capacity estimation focus on the generalization of existing methods and do not distinguish between their application conditions or scenarios. The current booming market of EVs also requires the practicality of onboard BMS. It is found that there is a lack of a summary of the existing knowledge for onboard capacity estimation. Therefore, this work overviews and compares the current battery capacity estimation methods suitable for onboard BMS. The characteristics of various capacity estimation are reviewed and discussed in this paper.

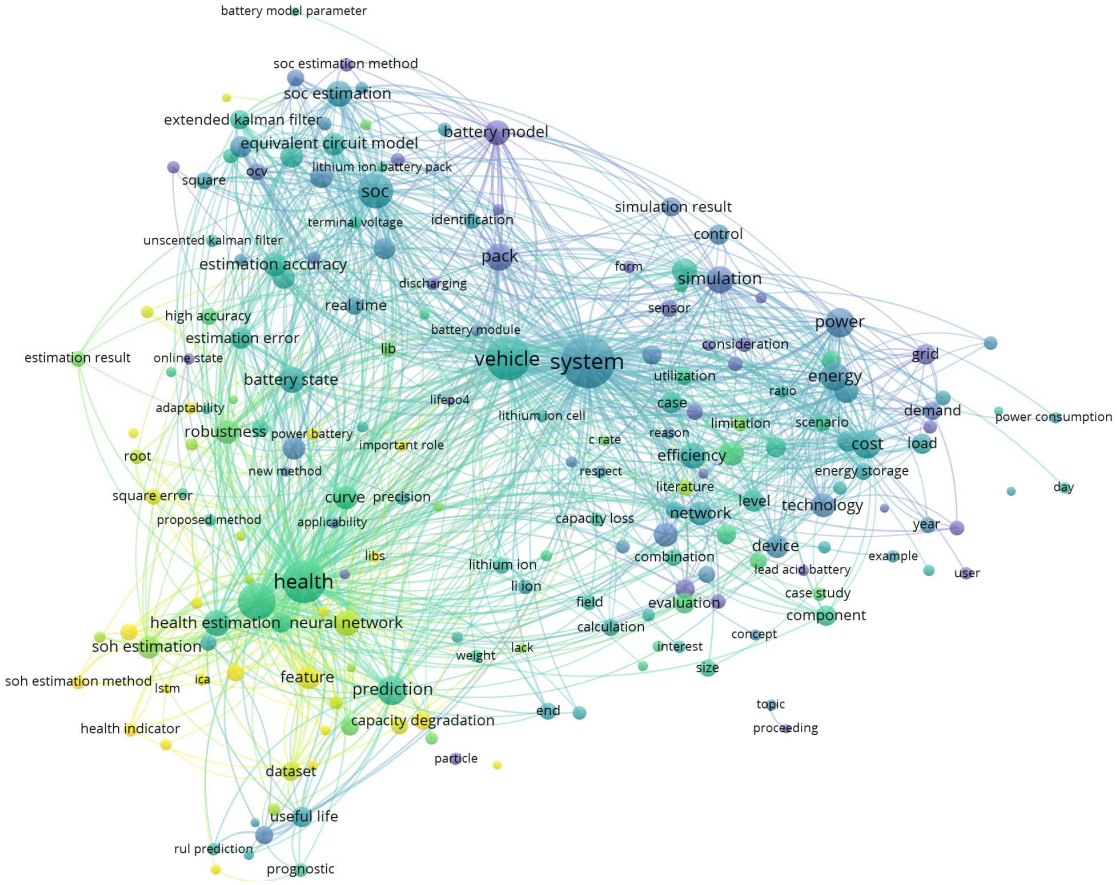

Figure 3. High-frequency keyword co-occurrence network for battery capacity on Scopus from 2016 to 2021.

The rest of this paper will be structured as follows: Section 2 briefly analyzes the battery degradation mechanisms. Section 3 reviews the existing methods for onboard battery capacity estimation. Discussion and perspectives are expressed in Section 4. Section 5 is the conclusion of this work.

2. Li-Ion Battery Degradation Mechanism Analysis

An Li-ion battery mainly contains the lithium metal oxide as the cathode, and graphite as the anode material at present. A separator exists between the two electrodes for insulation, which only allows the pass of Li-ions, and the electrons can only exchange through external circuits. Additionally, an electrolyte is also needed to assist the transfer of Li-ion. Thus, it is clear that the Li-ions exchange from the electrodes during battery charging and discharging [37]. For EVs, the reduction of the battery capacity results in less energy available, which directly reflects the performance degradation of the battery pack. The capacity loss of the battery is a non-linear process containing complex aging mechanism. However, the aging mechanism of batteries cannot be precisely described, especially for the decay rules of cycle life. To conveniently analyze the battery degradation, recent research usually divides the battery aging into two main forms: calendar aging and cycling aging [38–41].

Calendar aging refers to the capacity loss during storage, which is mainly influenced by high temperature and SOC [42–44]. Five aging cases are set in [43] for the calendar aging of 15 Li-ion batteries for a period between 24 and 36 months. The test results clearly prove there is a non-linear battery degradation during calendar aging, and the fading rate of the Li-ion battery is accelerated by increased storage temperature and SOC. Among all the influencing factors, high storage temperature is believed to be the most critical factor for battery calendar degradation [45,46]. LLI is the main reason for calendar aging with high temperature [15].

However, cycling aging is always accompanied by calendar aging in an actual application, which makes it complicated to clarify the degradation procedure. Cycling aging is the main reason for battery aging in BESS; Belt et al. [47] have tested 107 commercial cells and the results show that the charge-depleting by cycling aging is far more than the calendar one. Cycling aging is closely related to the charging and discharging process of Li-ion batteries. Chemical reactions are essential for the process of Li-ion movement between the electrodes [48]. Thus, the investigation of battery cycling aging needs to consider the current rate, Depth of Discharge (DoD) and SOC, etc. [49]. During cycling aging, the distribution of the current density, SOC and temperature is not consistent inside the cell as illustrated in [50]. The inhomogeneities of distribution in the cathode material will further induce mechanical force to fatigue the electrodes, and thus accelerate the battery cycling degradation.

It is clear that the Li-ion battery degradation is the coupling of multiple factors, as shown in Figure 4. The degradation modes of Li-ion battery are also LAM and LLI as previously described [51]. The thickening of a Solid Electrolyte Interface (SEI) and lithium plating in the graphite anode will both consume the lithium inventory, and thus results in the LLI of an Li-ion battery. No chemical reaction is ideal without any losses and generates some extra products. Thus, the reactions during cycling and storage cause the LAM of both cathode and anode. Both LAM and LLI are observed by the incremental capacity and differential voltage curves in LFP, LMO (Lithium Manganese Oxide) and LTO (Lithium Titanium Oxide) batteries according to the results in [52]. Inappropriate temperature ranges, overcharging or discharging, and high SOC (>80%) are the external factors which can speed up the battery aging process [53–55]. Complicated degradation behaviors of the battery make it difficult to clarify all the details in theory.

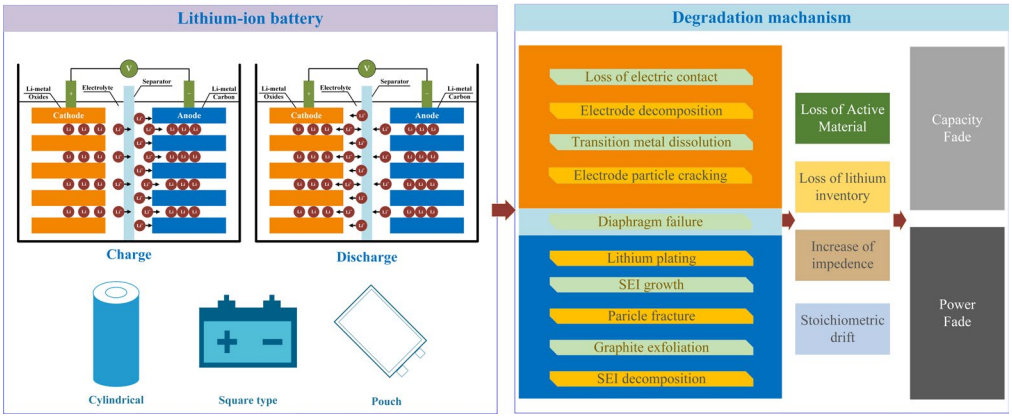

Figure 4. The effect of factors on the battery capacity degradation.

Here, we also illustrate the degradation measurement results of two commercial Li-ion batteries under calendar aging and cycling aging in Figure 5. With a higher storage temperature, the capacity of a battery in T = 45 °C decreases faster than 30 °C. It is also clear that the Li-ion battery charged with a larger current (2.7 C) degrades faster than with a lower charging C-rate (1.3 C). A Neware battery tester is used to cycle the battery, more details about the cycling aging setting can refer to [56].

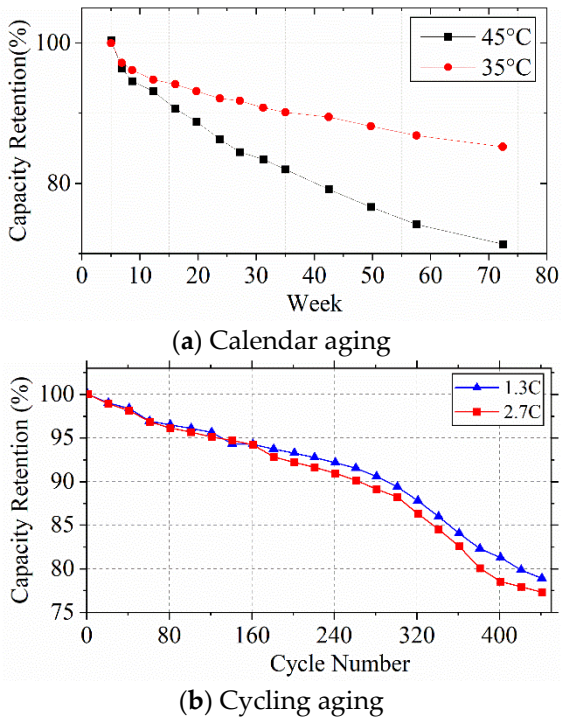

Figure 5. Li-ion battery degradation. (**a**) 36.9 Ah Li-ion batteries stored at SOC = 100% in thermostat (T = 35 °C, T = 45 °C), the capacities are measured every four weeks; (**b**) 1.5 Ah NMC based 18,650 Li-ion batteries are charged with 1.3 C and 2.7 C, and discharged by 5 C. The capacities are measured every 20 cycles.

3. Review of Capacity Estimation Methods

Considering the complexity of battery degradation, it is still challenging for the BMS to accurately predict the battery capacity onboard. Thus, researchers have made significant efforts to solve this problem. This section will brief introduces the battery capacity estimation methods in the literature. We mainly divide the methods into direct measurement methods, analysis-based methods, SOC-based methods and data-driven methods, whose principle and current processes will be detailed in the following subsection.

A. Direct Measurement Method

The most straightforward way to receive the battery capacity is to accumulate the charge during its cycling period [57]. Direct measurement methods need a full charge or discharge of the battery under a specific condition. Current various standards from International Electrotechnical Commission (IEC) [58], International Organization for Standardization (ISO) [59] and Institute of Electrical and Electronics Engineers Standards Association (IEEE-SA) [60] have been proposed for testing the Li-ion battery capacity in a standard condition. For example, ref. [58] defines a 1/3 I_t constant discharging current for EV and 1 I_t discharging current for HEV, for the purpose of measuring the battery capacity. As for the capacity measurement in [59], 1 C current is recommended for discharging the high power battery and C/3 is used for measuring high energy battery. It is not difficult to realize that the measured battery capacity may not be the same for different C-rates and temperature settings in those standards. In addition, the test procedure is rather strict compared with the working environment of the battery pack in a real application. [58] needs the battery soaked at a predefined temperature for at least 12 h to ensure thermal stabilization, which requires the cell temperature changes lower than 1 °C in 1 h time interval. The current and voltage measurement accuracy should be less than +/− 1%, and the time is measured less than +/− 0.1% in [59]. Thus, it is not practical to always meet the above requirements in a battery application, which limits these test methods to laboratory tests as references.

Another concern is that in reality, the BESS cannot always fully charge or discharge in various load conditions. Direct measurement methods cannot give a result if the battery is partially charged or discharged, which often happens in real cases. To clarify this point, an SOC profile of BESS for primary frequency regulation lasting one week [31] is shown below in Figure 6. Mostly, the SOC of the BESS varies within 40–60%, which confirms the unrealistic implement of direct measurement methods in a real application. It is noted that fully charging or discharging the battery is also quiet time-consuming [61].

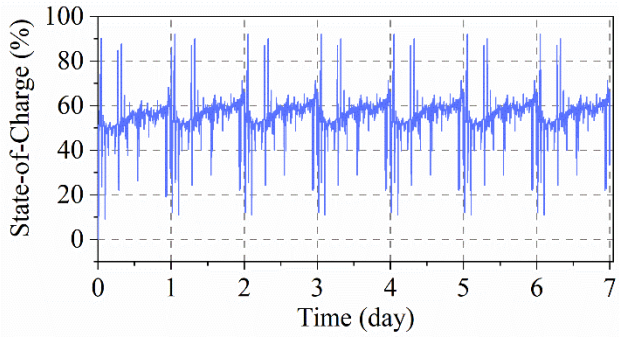

Figure 6. SOC profile of BESS for the primary frequency regulation of grid.

For convenience, an option is to measure the internal resistance to reflect the battery capacity. The battery internal resistance can be directly measured by applying a current pulse to the battery [62] as shown in Figure 7. Usually, the current pulse lasts a few seconds, and then the internal resistance can be calculated by the following Equation,

$$R_{bat} = \frac{\Delta U}{\Delta I} = \frac{U_A - U_C}{I_A - I_C} = \frac{U_B - U_D}{I_B - I_D} \quad (1)$$

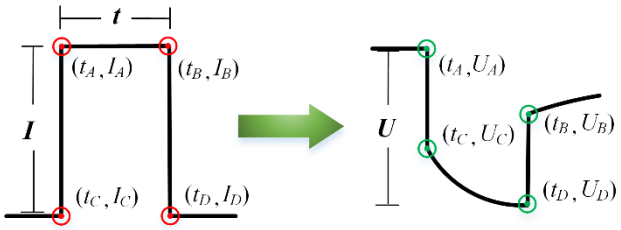

Figure 7. The DC internal resistance measurement for Li-ion battery.

Unfortunately, the internal resistance is more related to the power fade of the battery, which does not always exhibit a linear relationship with capacity fade. The capacity degradation is related to lithium corrosion at the anode, while the power fade is related to SEI growth and LAM [63]. Moreover, the internal resistance measurement is also affected by C-rate, temperature and SOC, and the internal resistance is quite small in the milliohm range [43,64,65]. Thus, some uncertainties may exist if only internal resistance is used for calculation. Direct measurement methods are strictly performed by charging and discharging of the battery in laboratories. As for onboard BMS implementation, the practical application requires estimation methods that can be done with limited complexity.

Therefore, more advanced methods are needed to estimate the battery capacity by processing the current, voltage, temperature and mechanical stress. Those existing methods include analysis-based methods, SOC-based methods and data-driven methods, which will be introduced in the following subsections.

B. Analysis-Based Methods

For indirect methods, the voltage, current and temperature can be recorded by sensors, and then used to estimate the capacity. In this work, we mainly introduce five kinds of analysis-based methods with IC (Incremental curve) curve, DV (Differential voltage)

curve, DT (Differential thermal) curve, mechanical stress and Electrochemical Impedance Spectroscopy (EIS) as shown Figure 8. At present, more attention is paid to the Li-ion battery capacity. The capacity, which limits the available energy, is the key indicator for State-Of-Health (SOH), which is defined as the ratio of current maximum capacity to its initial capacity [66].

$$SOH = \frac{Q_{present}}{Q_{initial}} \tag{2}$$

where $Q_{present}$ denotes the current capacity and $Q_{initial}$ is the nominal capacity. Thus, we will not distinguish capacity estimation and SOH estimation in the following explanations.

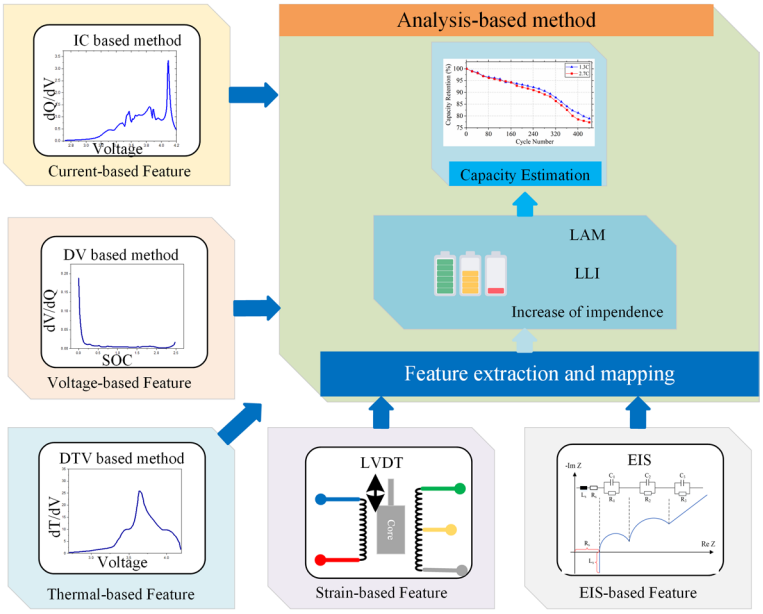

Figure 8. Schematic of analysis-based method.

(1) Incremental curve analysis method

IC curve analysis method focuses on the variation of capacity with voltage, which is expressed as,

$$IC = \frac{dQ}{dV} \tag{3}$$

In the IC curve, the dQ can be easily obtained by Coulomb counting of the current. Since noise always exists in current and voltage measurements, a filter is usually needed to smooth the IC curve [52,67,68]. Usually, a low-pass filter [69], Savitzky–Golay filter [70,71] and Kalman filter [72] have been used to process the IC curve for reducing the noise sensitivity. A two dimensional Luenberger–Gaussian-moving-average filter is designed in [68] to enhance the IC curve extraction. Once a smooth IC curve is obtained, the mechanisms of the Li-ion battery can be analyzed accordingly. The peaks and valleys in the IC curve are related to the voltage plateau of the battery. In [52], the degradations of three peaks in the IC curve are related to LAM and LLI, and the small shift of the IC curve indicates a slight increasement of the battery internal resistance. Then, the shape variation of the IC curve, especially, the peak and valley changes can be used for analyzing the capacity degradation trend and capacity estimation. The analysis procedure of the IC curve is summarized as Figure 8.

Since the insertion and extraction of Li-ions can change the phase transformation of the material in the electrodes, the IC curve is an effective tool to reflect the battery degradation. The LLI and LAM of six LFP batteries are quantitatively analyzed by the IC curve in [73] for the battery health diagnosis, which utilizes the heigh, area, shape and position of the five peaks in the IC curve. A regression model can be then easily established by using the variations of the IC peak. A linear regression model characterized by ordinary least squares

is used for battery health estimation in [73]. Ref. [74] also uses the IC peak as the feature for battery capacity estimation, which chooses the grey relational analysis as the estimator and the maximum error is claimed less than 4%. Utilizing the IC peak and the related area, the capacity of the retired battery is also evaluated in [75]. A IC curve based mode is proposed in [76] to describe the phase transition behavior of active material of a Li-ion battery, which is used for battery capacity estimation and later verified on LFP, NMC, LTO chemistries. The proposed model has also claimed to reduce noise from sampling and measurements, which is suitable for onboard BMS.

The IC curve mainly extracts the variation of the voltage with Li-ion battery degradation, and thus can be used for aging mechanism analysis. However, a very low current rate is needed to obtain the IC curve for battery diagnosis, such as 1/10 C in [45]. Analyzing the battery degradation with IC curve also requires specialized knowledge of the electrochemical reactions inside the battery.

(2) Differential voltage curve analysis method

DV curve [77] is quite like IC curve in analysis, which is described as,

$$DV = \frac{dV}{dQ} \tag{4}$$

From Equation (4), we understand that the DV curve can also be obtained from the current and voltage measurements during charge or discharge. The basic idea to analyze the degradation of a battery cathode and anode is based on the variation of the DV curve [78]. The battery capacity can be also deduced from the trend of the variation in DV curves. Despite the requirement of a smooth filter, some publications also choose DV curve as a tool for capacity estimation. Ref. [79] measures the DV curve of a half-cell, and investigates the DV curves of positive and negative electrodes, respectively. Features of DV curve related to LAM and LLI are used for battery degradation estimation. The DV curve changes of a LTO battery is discussed in [80] to analyze the aging mechanism during a number of 1080 cycling tests. The aging modes of positive and negative electrodes are expressed by the peak and valley of DV curves, which can be further used as the reference for the degradation information extraction from a Li-ion battery. A comparison of IC and DV curves is studied in [52] for the aging mechanism identification of five commercial Li-ion batteries, and experimental results prove the good consistency of IC and DV curve in battery degradation mode analysis. In short, using a DV curve for battery capacity estimation is similar to an IC curve; both utilize the variation of the curve's shape to analyze the aging mechanisms and then extract features as the input of a regression model for capacity estimation. The characteristics of the DV curve can also refer to the IC curve in the previous section. We have to mention that one good advantage of those methods is the use of direct measurements from BMS which is low cost to implement. A common challenge is to deal with the measurement noise in reality [81].

(3) Differential thermal analysis method

Considering that the general measurements from BMS contain current, voltage and temperature, the differential thermal voltammetry [82] is chosen to diagnosis the Li-ion battery degradation as,

$$DT = \frac{dT}{dV} \tag{5}$$

There always is heat generation during the battery operation, which is divided to reversible and irreversible heat. The reversible heat is generated by the entropy change of the electrochemical reaction in electrodes, while irreversible heat is mainly the ohmic resistance heat, polarization heat and the side reactions heat [83]. Those thermal characteristics are also charged with battery degradation. Therefore, it is possible to use the temperature variation during charge or discharge as the indictor for battery capacity estimation [67,84,85]. Here, we plot the DT curve of the Oxford dataset [86] as shown in Figure 9, which indicates a variation on the peak and valley with the increase of the cycling number.

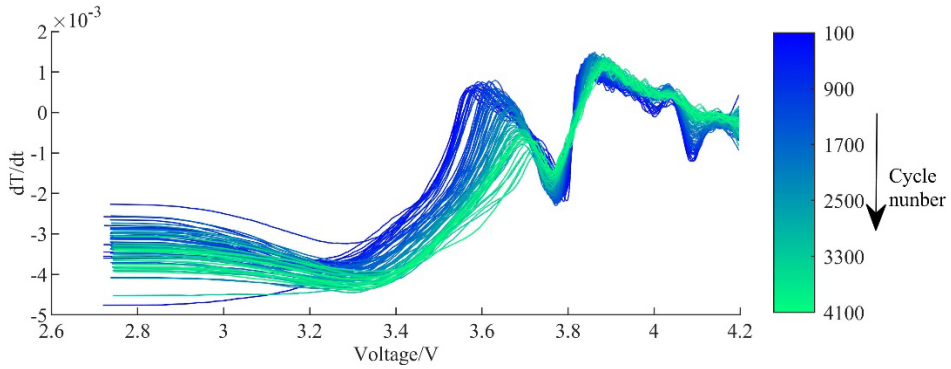

Figure 9. DT curve of the Li-ion battery cell in Oxford dataset.

The DT curve of LCO and NCA batteries are analyzed in [85], and the peak and valley of the DT curve can be used for capacity estimation. The position of the peak and valley in the DT curve is selected as the features for a Gaussian Process Regression (GPR)-based data-driven estimator in [87]. Both IC and DT curves are analyzed and compared, which shows that the MAE of DT curve is 19.50% less than IC curve on Oxford and NASA dataset [88]. Ref. [89] extracts the temperature variation during a 1 C constant current charge process, the time interval of two temperature cooling areas are selected as the feature for capacity estimation on both calendar aging and cycling aging.

Compared with IC and DV curves, the DT curve can be suitable for high current charge or discharge. However, the DT curve is also sensitive to measurement noise. The DT curve can be used for aging mechanisms analysis because it is essential the heat generation during the electrochemical reactions. In addition, the connections of the DT curve to battery aging still need to be investigated.

(4) Mechanical stress analysis method

The volume of the particle will change during the charge or discharge of an Li-ion battery. Taking an LFP battery as an example, the LFP particle expands by 6.77% during lithiation [90], while the intercalation of Li-ion in the anode leads to 12% changes in the volume of graphite [15]. Thus, it is reasonable to use the mechanical stress for battery performance analysis [91–93].

It is proved in [94] that the thickness of the Li-ion battery varies by 54.5 µm after the first discharge and the changes of the thickness is 13.5 µm after ten full cycles for a 60-Ah NMC Li-ion battery. It is clear that the mechanical stress of the Li-ion battery will change both with SOC and battery aging. The swell of a commercial 5-Ah Li-ion battery is investigated in [95], where the relationship between the battery swelling and C-rate, SOC and temperature is analyzed. Especially, the authors claim that the ds/dQ can be used for identifying the phase transition in the negative electrode, and further acts as the tool for aging estimation. Ref. [96] proposes a force-based incremental capacity analysis method for Li-ion battery capacity fading estimation, which detects the expansion force of a MNC cell from a HEV battery pack. The experimental results have proven that the proposed method is better than IC curve in signal-to-noise ratio. A high relevance of the second derivative of strain and IC curve are found in [97], where the strain of the electrode can be used for the state estimation as IC curve. The results also prove the second derivative of strain is less sensitive to C-rate compared with IC method, which is expected to be more suitable for real battery-based applications.

Although mechanical stress is believed to be an effective way for battery detection, the main limitation is the requirement of a specially designed device for swell measurement such as displacement sensor, pressure sensor, test fixture, etc. In this way, the cost is increased and also its implementation to a battery pack must be carefully considered for not destroying its original design.

(5) EIS analysis method

EIS is an effective tool with high sensitivity to the electrochemical reactions inside the Li-ion battery; it has been used for battery modelling [98,99], SOC and temperature estimation [100], and also battery degradation diagnosis [101,102]. Generally, EIS is measured in the battery equilibrium state with small current or voltage injection in a frequency range between mHz and kHz [103]. The real and imaginary parts of impedance measurement is selected as the input of a Gaussian Process Regression (GPR) model for Li-ion battery capacity and RUL estimation, in which the variation of EIS with battery degradation is shown in Figure 10. The EIS curve turns from blue to red with battery aging. Ref. [104] combines EIS with ultrasonic time-of-flight analysis to investigate the electrochemical characteristics and structure variation inside a Li-ion battery when the cycle number of a battery increases. Refs. [105,106] extract the parameters of ECM from EIS curve, and then analyze the connections between the parameters and battery aging for estimating the battery capacity. [107] uses S transform to a fast calculation of battery impedance, and the zero-crossing point of real impedance R0 is chosen for battery capacity estimation.

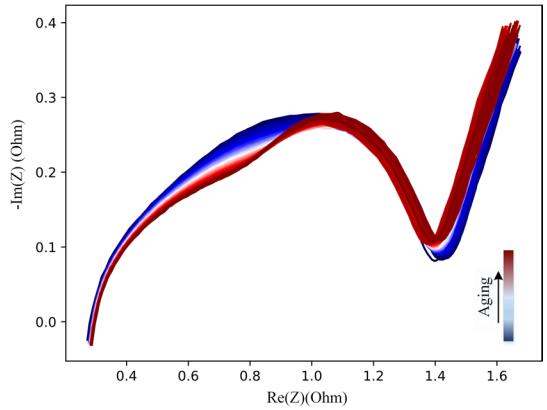

Figure 10. The variation of EIS with Li-ion battery degradation with data from [101].

Battery EIS has a strong potential to reflect the electrochemical reactions in the frequency domain, which is expected to have great potential for onboard BMS application. However, most EIS related battery degradation analysis are based on the commercial electrochemical workstation which is accurate yet expensive. Considering the volume and weight of the electrochemical workstations, they are difficult to be directly used in an EV environment. Therefore, two kinds of solutions have been proposed recently to address the issue of EIS measurement with BMS and machine drive electronics. One method is to combine with the onboard chargers [108] or DC–DC converters [109,110]. An onboard charger is integrated with a Dual Active Bridge (DAB) converter for charging and EIS measurement of the battery pack in EV [108]. The second method is using low power measurement module in a BMS for small AC signal injection. [111] uses Single-Cell Supervisor (SCS) designed by NXP Semiconductors injecting the AC current to the battery, and the battery impedance can be calculated by measuring the voltage response. However, there are still very limited examples on hardware design of EIS measurement [112] considering the cost of current BMS. Another concern is that the measurement of EIS is easily affected by noise which hinders a reliable usage of EIS on battery capacity estimation.

C. SOC-based method

An SOC-based methods can be divided into SOC indirect estimation and the SOC observer-based method, which is illustrated in Figure 11. SOC indirect estimation calculates the battery capacity through a period of Coulomb counting and SOC variation, which usually estimates the battery in a short time scale online. The SOC observer-based method directly estimates the battery capacity utilizing an observer based on battery Equivalent Circuit Model (ECM) model, which uses only current and voltage as the input, and SOC and capacity can be estimated synchronously.

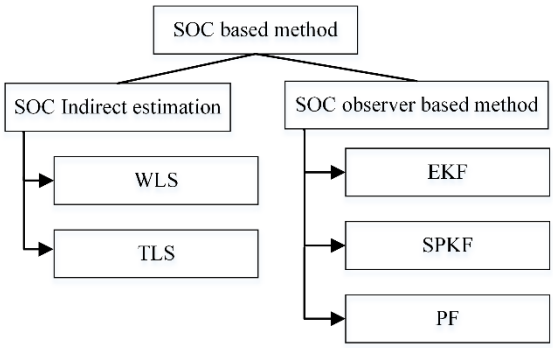

Figure 11. SOC-based method.

(1) SOC indirect estimation

SOC indirect method is essentially based on the coulomb counting equations, which is expressed by the following equation,

$$SOC(t_2) = SOC(t_1) + \frac{1}{Q}\int_{t_1}^{t_2} \frac{\eta i(t)}{3600} dt \quad (6)$$

where η is the coulomb efficiency, $i(t)$ is the current, and Q is the capacity. From Equation (5), the battery capacity can be calculated once the SOC variation is known.

LS is a commonly used method for parameter estimation of a linear model, which offers a mathematical model to fit the experimental data with a minimum residual sum of squares errors [113]. According to Equation (6), the capacity can be solved by linear regression with SOC and current information.

Weighted Least Squares (WLS) is calculated by considering the weights of the data based on an ordinary LS [114]. Based on the linear function structure $y = Qx$, where y is measurement, and x is an independent variable. In this case, the model can be expressed as $Y = y - \Delta y = \tilde{Q}X$ as shown in Figure 12a, where Y is the measurement vector and X is the independent variable vector, and the measurement errors Δy is considered as the weightings. Ref. [115] uses the errors from the observations as the weights to calculate a fitting equation. Capacity is set as a time-varying parameter and then solved by a recursive approximation [116].

(**a**) WLS (**b**) TLS

Figure 12. Data errors on two LS-based method.

Ref. [117] proposes a capacity estimation algorithm based on LS methods for PHEV and EVs. With the given current signal, the OCV is calculated by LS and the relationship between SOC and OCV is mapped. Then capacity is obtained by the iteration process. Wei et al. [118] propose an SOC and SOH estimation based on two LS estimators. Under the condition that no pre-determined parameters are necessary, OCV is derived by LS estimator, and then the capacity is converted to linear fitting problem to solve according to the mapping relationship between OCV and SOC.

Total Least Squares (TLS): During the calculation of ordinary LS, it assumes that the input data are accurate, but in actual operation process, the input and output data are both influenced by measurement noise. Presented in terms of data fitting, WLS only accounts for Δy, while Total-Least-Squares (TLS) accounts for both Δy and Δx. Therefore, TLS is

introduced for capacity estimation, considering the disturbances from both input and output [119,120]. In this way, the model can be expressed as $Y = y - \Delta y = \widetilde{Q}X = \widetilde{Q}(x - \Delta x)$ in Figure 12b, where Δy is the measurement errors and Δx is the input data errors. The TLS problem can be solved by a singular value decomposition of the matrix, but the multiplier of the singular value decomposition of the n × n matrix is $6N^3$ [121]. After analyzing the calculation of TLS, Rhode et al. [122] find that it is difficult to derive an analytical solution to the matrix and therefore they propose a recursive form to solve the TLS problem and satisfactory estimation results are finally obtained. Ref. [123] uses the constraint Rayleigh quotient as the cost function in the TLS calculation process, which greatly reduces the complexity of the TLS.

(2) SOC observer-based method

The SOC observer-based method attempts to estimate the battery capacity according to the SOC estimation results in a dual time scale framework.

As for the SOC observer-based method, the capacity estimation is developed based on ECMs. The ECMs describe the external characteristics of the Li-ion battery using resistance, capacitance, and voltage source as shown in Figure 13 [124]. It is believed that the complexity of ECMs is suitable for online BMS applications [125]. Depending on different numbers n of the RC networks, which describe the dynamic characteristic including the polarization characteristics and diffusion effects [126], the Rint model (n = 0), Thevenin model (n = 1), and dual-polarization model (n = 2) are proposed, respectively [127].

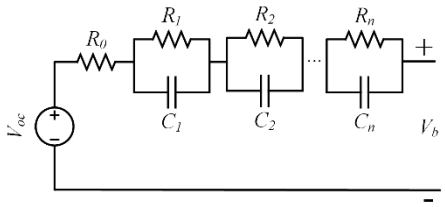

Figure 13. ECM with n-RC.

In existing studies, capacity is often considered as one of the parameters to be estimated in parallel with another battery state such as SOC [128]. This is also known as joint estimation [129]. Based on the coulomb counting Equation (2), SOC estimation and capacity estimation are coupled. In the joint estimation of SOC–SOH, capacity as a dynamic parameter is treated as an extended state of the filter, and then parametric filtering is performed [130,131]. For filters, there are two core components, prediction, and correction. Predicting the state from the previous moment and correcting the result based on the observations, the prediction and correction are continuously recursive to complete the estimation of the state. Figure 14 is a schematic diagram of the filtering process using the Kalman filter as an example [132,133]. The equations for a stochastic linear discrete system are described as:

$$x_k = Ax_{k-1} + Bu_k + \omega_k \tag{7}$$

$$y_k = Hx_k + v_k \tag{8}$$

where x is the state vector, A is the state transfer matrix, u is the state control vector, B is the control variable matrix, y is the measurement vector, H is the transformation matrix from the state vector to the measurement vector, w and v are both noises obeying a Gaussian distribution, and P is the covariance matrix.

Extended Kalman Filter (EKF): KF is somehow limited to linear systems [134]. In ref. [135], the researcher linearizes the non-linear OCV–SOC curves into seven segments to meet the requirements of KF for a linear system model. However, in the case of long-term battery capacity decrease, as mentioned in Section 1, the degradation process is of much nonlinearity. Thus the improved KF-based EKF is a better choice for achieving battery capacity estimation [136]. Ref. [137] proposes a co-estimation of multiple battery states using the correlation of parameters in the state space. Based on the EKF for SOC estimation and cumulative charge, the battery capacity is solved simultaneously. Ref. [138] proposes a

dual filter of state and parameter based on EKF to achieve a simultaneous estimation of SOC and SOH. The parametric filtering is used to update the capacity online to improve the accuracy of SOC estimation.

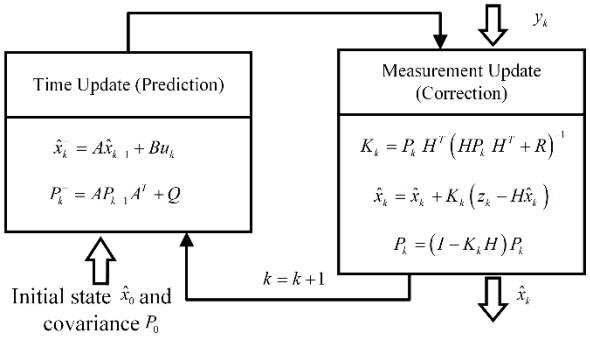

Figure 14. Filtering process of Kalman filter.

Sigma Point Kalman Filter (SPKF): For those situations where the degree of nonlinearity is higher, SPKF is a better choice. SPKF is an improvement of KF without linearization steps or computing the derivatives [139]. The mean and covariance are obtained by a set of weighted points passing through the non-linear function. According to the pattern of choosing the sigma points, SPKF is divided into Unscented Kalman Filter (UKF) [140] and Central Difference Kalman Filter (CDKF) [141]. Compared with EKF, SPKF avoids the necessity of complex differential processes and has a better covariance approximation. However, under more frequent current fluctuations conditions, its accuracy and stability still cannot be guaranteed [142]. Ref. [143] proposes a UKF-based dual filtering framework based on the coupling of SOC and capacity as shown in the coulomb Equation (6). Real-time capacity is updated as recursive filtering of SOC state and capacity parameter proceeds. Ref. [144] presents a joint estimation for multiple critical states along with an autoregressive equivalent circuit model. The state space-coupling model is solved using UKF which has good dynamic tracking properties for multiple states.

Particle Filter (PF): PF is commonly seen in tracking the capacity in the full lifespan of a battery [145–147]. By employing the Monte Carlo sampling techniques, PF offers the possibility of dealing with any type of distribution by a proper group of particles or samples approximating the respective probability density functions [148]. Ref [149] uses an optimized dynamic single exponential model to describe the degradation of capacity and particle filtering to complete the optimal state solution. The performance of single-step, multi-step and long-term capacity prediction based on particle filtering is analyzed in detail.

It is noted that the time scales of state and parameters changes are different [150]. Typically, the time scale for SOC changes is much smaller. In [151], the time scale of SOC is set as 1s, while capacity is 60s. Thus, the two variables are filtered separately by independent filters. In addition, in the common joint SOC–SOH (denoted by capacity) estimation, the coupled nature of the state space equations requires a high degree of accuracy for both estimators. Otherwise, the cross-interference between the two will become a difficult problem for the joint estimation. i.e., SOC and capacity uncertainties can interfere with each other in the process of information exchange. Ref. [152] proposed the decoupling of parameter identification and state estimation. The capacity identification estimator is fully decoupled from the SOC state estimator. Different time scales are adopted to further improve the accuracy of the results.

As we can find for the SOC-based method, accurate SOC is the important prerequisite for capacity estimation. However, SOC itself is not an easy measurable status for the Li-ion battery, which limits the usage of SOC-based methods in reality.

D. Data-driven method

With the fast development of IoT and artificial intelligence, the daily operation measurement of the battery system is easy to be recorded to a cloud platform which could be further used for cloud to edge estimation. The data-driven approach is characterized by a reliance on a large amount of dataset to make decisions and does not require a specific battery model. In a data-driven approach, a model can be used to map the data as long as a sufficiently representative sample is available, without the need to pre-determine a definitive model in advance. In the case of batteries, the operation measurement that we can collect may contain aging information. The degree of aging can be reflected by certain characteristics during the charging and discharging process, and the data-driven approach constructs an approximate model to match the true aging situation with this information. Figure 15a is a schematic diagram of the data-driven approach application procedure, which mainly includes three processes: data collection & preprocessing, offline training and online estimation. The main purpose of data collection is measuring the voltage, current and temperature during the operation of the battery pack. Then, the data-driven model can be trained offline with high computing power processor, and the trained model is later implemented in a BMS for online estimation. In this type of method, the keys lie in the processing of the data, the extraction of key features and model training, the main data stream of those processes is shown in Figure 15b.

The existing data-driven method is introduced in the following subsections.

Neural Network (NN): The basic NN is a three-layer structure network including an input layer, hidden layer and output layer. The input layer neuron can be regarded as extracting capacity-related features [153]. It is critical to choose a suitable indicator. Refs. [154,155] use NN to investigate the battery capacity. From the perspective of feature extraction, the former uses discharge voltage, while the latter adds also the temperature effects. The weight coefficients from the input layer to the hidden layer or from the hidden layer to the output layer need to be obtained after training a large number of samples [105]. Ref. [156] chooses to train a generalized regression NN with the battery's constant current charging time to estimate SOH. The instantaneous discharging voltage drop and the amount of Ah-throughout for a certain depth of discharge are captured as features. Ref. [157] uses the Broad Learning System (BLS) to process historical capacity data and generate feature nodes as the input layer of the neural network. This method does not require an in-depth study of the battery aging mechanism, but it also requires at least 25% of the historical capacity data.

Support Vector Machine (SVM): Support Vector Machine (SVM) is another technique. The core is to divide the data set in a hyperplane [158,159] so that the geometric interval between each data point can be maximized in the hyperplane. It can be transformed into an objective function under constraints to solve the optimization problem. Ref. [160] studies the relationship between the electrolyte concentration and voltage with the battery capacity. The non-linear relationship is then fitted by SVM. A Least Squares Support Vector Machine (LSSVM) is used in [161], with charging voltage, discharging current, temperature, and cycle times as inputs, and the residual sum of squares error is selected as the cost function to calculate the capacity retention rate. Ref. [162] uses Particle Swarm Optimization (PSO) to find the suitable hyper-parameters for the SVM kernel function and trains the impedance values as the features to complete the battery SOH estimation.

Bayesian learning method: Bayesian methods solve the posterior information with assumed prior probabilities to infer the unknown parameters [163]. There are a variety of data-driven methods that use their associated theory, such as the Relevance Vector Machine (RVM), which provides an output of posterior probabilities based on a Bayesian approach. Compared to SVM, it eliminates the need for model selection, but it often requires more training time. The literature uses empirical modal decomposition for battery capacity data, and sets up a multi-start prediction matrix to train RVM. It reduces the stochastic uncertainty associated with the starting point of a single prediction and parameter settings. GPR is derived from the Bayesian framework [164], and uses the Gaussian process prior knowledge to perform regression analysis on the data. Ref. [165] uses voltage segments in

short periods during constant current operation as the input of GPR for capacity estimation. The non-parametric regression properties of the GPR technique allow the estimation to be adapted to the complexity of the data.

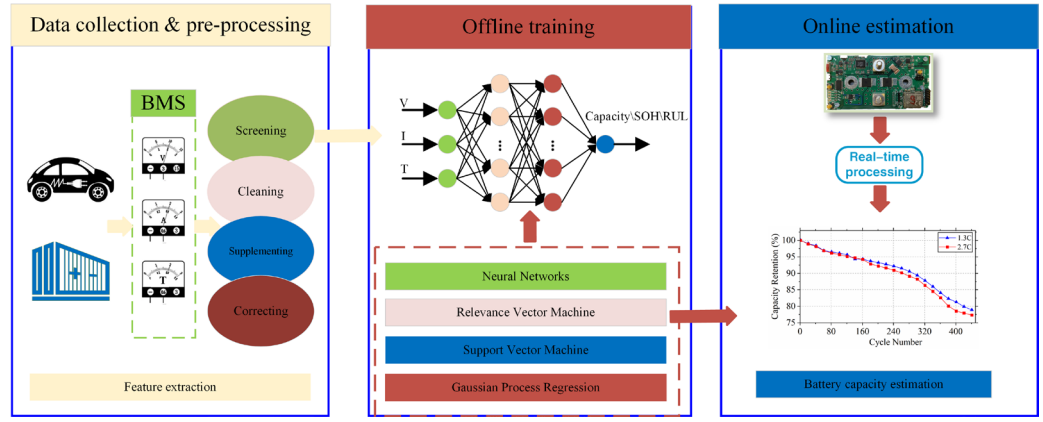

(**a**) Algorithm application procedure

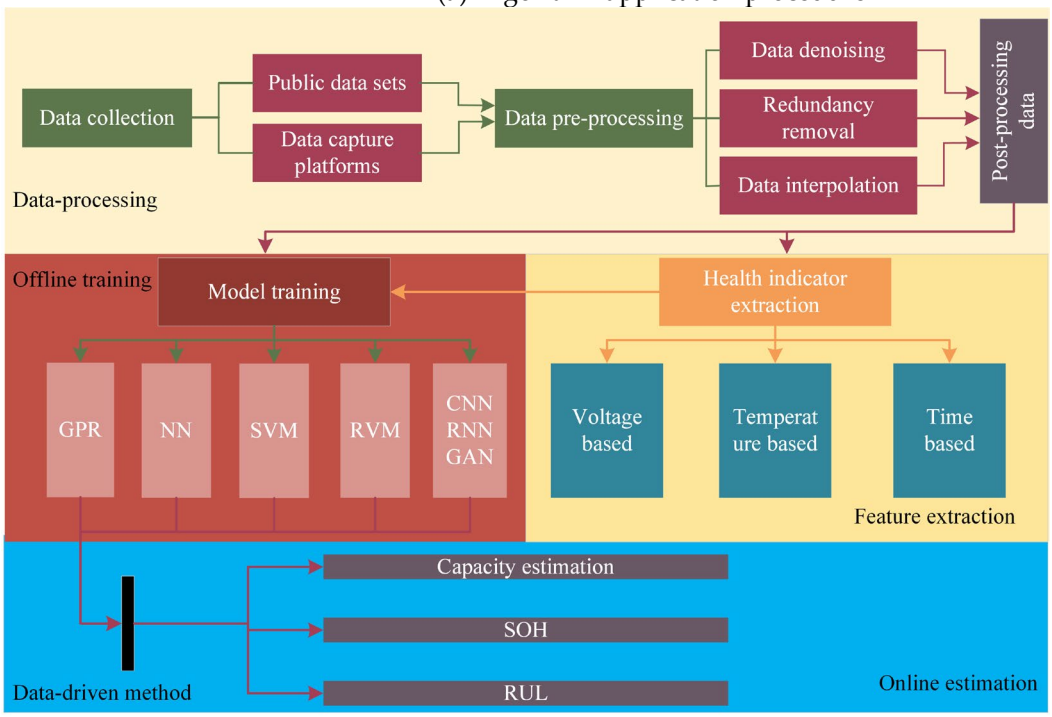

(**b**) Schematic diagram of the calculation process

Figure 15. The basic process of the data-driven approach.

Deep learning method: Deep learning utilizes multiple hidden layers in the network [32], which can reflect more complex mapping between the features and battery health. Methods, such as Convolutional Neural Network (CNN) [166,167], Recurrent Neural Network (RNN) [168,169] and Long Short-Term Memory (LSTM) [170,171] have been used for battery SOH estimation recently, and have shown promising performance in estimation accuracy. Ref. [167] takes advantage of CNN and Transformers for accurate SOH estimation of Li-ion batteries, which utilizes the attention mechanism to extract more important features from the original measurement. A differential evolution grey wolf optimizer is used in [171] to tune the hyperparameters of LSTM for an accurate battery health estimation. A hybrid of gate recurrent unit and CNN is shown to estimate the Li-ion battery SOH in [172], which utilizes voltage, current and temperature as the input of the network.

The implementation of data-driven methods relies on the validity of the data and a complex training process. The advantage is that the model can be adapted to the data through training, but this also means that a large sampling and training dataset is required to achieve an accurate estimation.

4. Discussion

From the previous description, there have been a large number of studies on battery capacity estimation. We realize that some methods require specific implementation conditions. This paper discusses current battery capacity estimation methods for online BMS implementation, which are briefly divided into: direct measurement methods, analysis-based methods, SOC-based methods and data-driven methods. Since direct measurement methods are mostly limited to laboratory tests as a reference, the other three kinds of methods are compared with pros and cons in Table 1.

Table 1. A comparison of capacity estimation methods.

Methods	Examples & Relevant References	Estimation Error	Strength	Drawback
Analysis-based method	IC curve [67–76]	Max relevant error [4%] RMSE [0.0066–0.0605]	Reflect the chemical characteristics of the battery, Simple model structure	Noise sensitivity
	DV cure [77–81]	Max relevant error [3%]		
	DT cure [82–89]	Max relevant error [5.9%] RMSE [0.0027–0.0251]		
	Mechanical stress [90–97]	Max relevant error [12%]		
	EIS [98–112]	Max relavant error [2.2%] RMSE [0.0098–0.0116]		
SOC-based method	WLS [114–118]	Max relevant error [1%]	Less computation, Easy for online imply	Difficult to cope with complex non-linear problems
	TLS [119–123]	Max relevant error [0.15%]		
	EKF [134–138]	Max relevant error [0.5%] RMSE [0.0306–0.0599]	Closed-loop error management, Real-time dynamic tracking, Effective to handle the noise, Non-linear systems applicable	Complex model and parameter building process, High dependency on models,
	SPKF(UKF) [139–144]	RMSE [0.002–0.1275]		
	PF and their variants [145–149]	Max relevant error [0.4%] RMSE [0.0019]		
Data-driven method	NN [153–157]	RMSE [0.0121–0.0223]	No need to focus on internal mechanisms, simple model building, high adaptive capability, Powerful approximating ability, Non-linear systems applicable	High level of data dependency, offline training needed, Large computation effort, Over-fitting
	SVM [158–162]	RMSE [0.03–0.07]		
	Bayesian method [163–165]	Max relevant error [3%] RMSE [0.0041–0.0068]		
	Deep learning method [166–172]	Max relevant error [5%] RMSE [0.0032–0.0653]		

Analysis-based methods utilize the electric, thermal and strain characteristics of an Li-ion battery during charge or discharge, which always need a high precise sensor for measurement. The relationship between the analyzed physical quantity and battery degradation is closely related to measurement conditions and the materials of the battery chemistry; such factors limit the usage of the analysis-based method. In addition, professional knowledge is required to use curves for degradation mechanism analysis. IC and DV curves need to measure the voltage and current with high accuracy and low C-rate. All the analysis-based methods should be processed by a specially designed filter for receiving a smooth curve. The DT curve and mechanism strain are affected by various factors, such as the thermal management and structural design of the battery pack. The positions of the thermal and strain sensors in the battery module are still challenging, which limit their current usage in BMS products. Further investigations of the DT curve and mechanical stress are still needed to clarify the variation of the thermal and mechanical characteristics with battery degradation. EIS can detect the electrochemical kinetics inside the Li-ion battery with a small AC signal injection, which can reflect the battery degradation degree by the battery impedances, such as Ohmic resistance, polarization resistance, and SEI film resistance. With a broadband signal injection, the status of Li-ion battery can be analyzed in the frequency domain. Recently, some chips (DNB1168 [173]) have been made for EIS measurement of Li-ion batteries, which push the application of EIS to BMS a promising solution for the next generation BESS.

SOC-based methods rely on an accurate battery model. Although ECMs have been proven to have a good balance of accuracy and complexity, they are still far from been satisfied usage in a BMS. If the battery model is not reliable, the SOC estimation error will later affect the capacity estimation. In addition, the SOC-based methods usually obtain the results by iterations, which consumes the computing resources of BMS hardware. Thus, the application of SOC-based method will increase the cost of BMS. How to improve the computing efficiency and modeling accuracy still needs more further studies.

Data-driven methods treat the Li-ion battery as a black box without the need to deal with the complicated degradation mechanisms of the battery. However, quiet few data-driven models have been used in the current BMS. One reason is that the performance of the data-driven method is closely related to the feature and quality of the measurement dataset. There is a lack of open source datasets from a real BESS application for training the data-driven model. In reality, it is also difficult to obtain a labelled dataset, and measuring all the needed dataset from experimental testbench is costly. Another point is that the data-driven method lacks interpretability, and the credibility of the estimation results may be doubtful for real applications. The training of the data-driven model is closely related to a proper setting of the training procedure, while the training process is also time consuming. However, with the fast development of IoT and AI, data-driven methods will probably play a critical role in the future BMSs.

One key point we have to mention here is the materials of the electrodes might affect the applications of the capacity estimation methods for an application. For example, the NMC and LFP based battery characterize by a different OCV–SOC profile. The flat voltage curve of LFP battery corresponding to SOC may influence the capacity estimation accuracy. Thus, special attentions have to be paid when extracting features from the flat voltage curve or using OCV as the input of the method. IC curve can reflect the phase transitions of the electrodes, and probably can be used for feature extraction instead of a flat voltage curve for LFP battery.

We believe that the future onboard capacity estimation framework will be a hybrid of data-driven methods and other techniques as shown in Figure 16. Analysis-based methods can provide health features for the data-driven model. In this way, using an analysis-based method only needs a data processing procedure, and professional knowledge from the Li-ion battery degradation can be ignored. An SOC-based method can also be running in the BMS terminal, and can later collaborate with data-driven method through a fusion mechanism.

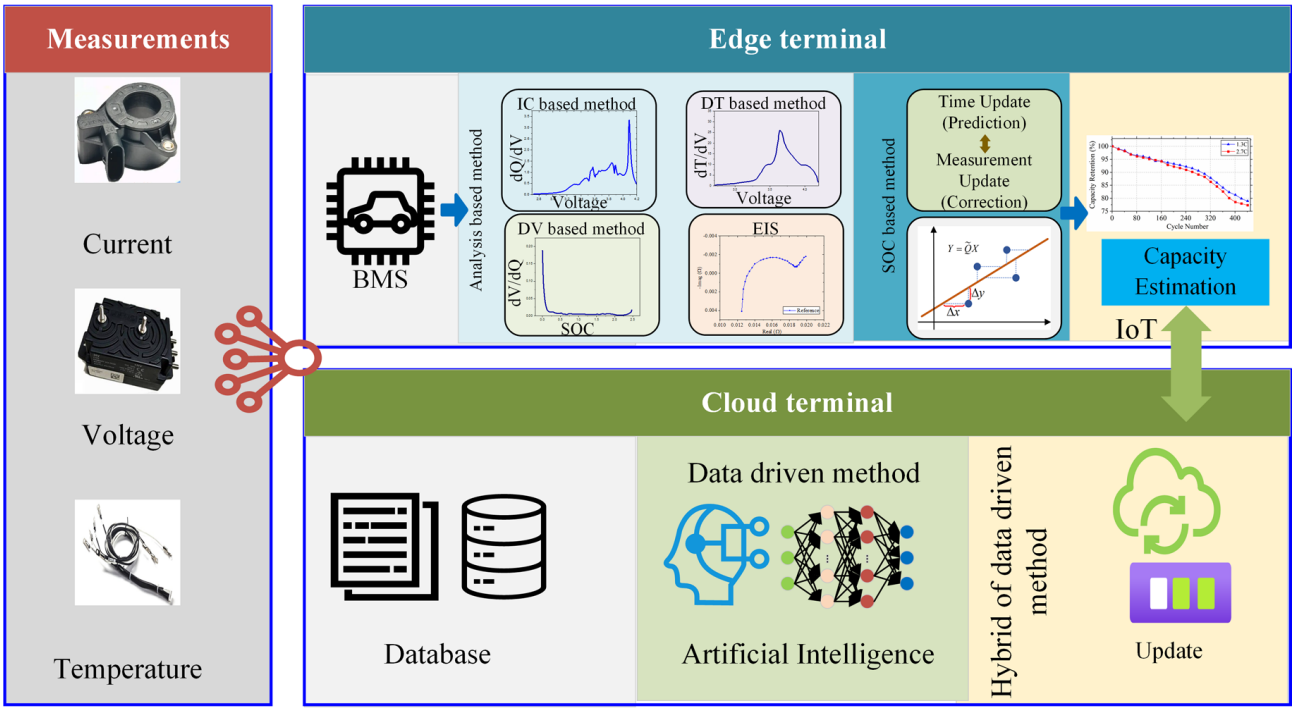

Figure 16. The prospective of future onboard capacity estimation framework.

5. Conclusions

This paper discusses a variety of methods for onboard BMS capacity estimation, which are based on different principles. These methods are divided into four main categories, direct measurement methods, analysis-based methods, SOC-based methods and data-driven methods. With emphasis on the onboard BMS implementable methods, the characteristics of each method are reviewed and discussed. Analysis-based methods with IC/DV/DT curves and mechanical strain are suitable for Li-ion battery degradation mechanism investigation. IC and DV curves are easier to be applied to a BMS application since no more sensor or measurement devices are needed in the battery packs. EIS is a promising solution for onboard BMS usage in the near future with an update of the hardware. SOC-based methods rely on the accuracy of the battery model and the iterative process requires more computing resources from the microprocessor in a BMS. With the development of the cloud-to-edge technique, data-driven methods will play an important role in the next-generation BESS.

From the methods discussed in this work, we hope to have summarized the recent progress in the battery capacity estimation area. In the future, a hybrid of various methods could be a more practical solution for real BMS applications, especially, a combination of data-driven and analysis-based methods.

Author Contributions: Conceptualization, J.P., J.M.; methodology, J.P., J.M.; software, J.P., J.M. and D.C.; validation, X.D., D.C. and X.S.; formal analysis, J.P., X.D.; investigation, J.M., D.C.; writing—original draft preparation, J.P., J.M.; writing—review and editing, J.P., J.M.; supervision, S.H., H.L. All authors have read and agreed to the published version of the manuscript.

Funding: This work is supported by the University-level Research Foundation of Nanjing Institute of Technology under grant YKJ2019114, the Open Research Fund of Jiangsu Collaborative Innovation Center for Smart Distribution Network under grant XTCX202005, and the National Natural Science Foundation of China under Grant 52107229.

Data Availability Statement: Not applicable.

Conflicts of Interest: The authors declare no conflict of interest.

References

1. Tang, C.Y.; Chen, P.T.; Jheng, J.H. Bidirectional Power Flow Control and Hybrid Charging Strategies for Three-Phase PV Power and Energy Storage Systems. *IEEE Trans. Power Electron.* **2021**, *36*, 12710–12720. [CrossRef]
2. Ku, T.T.; Li, C.S. Implementation of Battery Energy Storage System for an Island Microgrid with High PV Penetration. *IEEE Trans. Ind. Appl.* **2021**, *57*, 3416–3424. [CrossRef]
3. Matthew, T.L.; Suthar, B.; Northrop, P.W.C.; De, S.; Santhanagopalan, S.; Subramanian, V.R. Battery Energy Storage System (BESS) and Battery Management System (BMS) for Grid-Scale Applications. *Proc. IEEE* **2014**, *102*, 1014–1030.
4. Bharatee, A.; Ray, P.K.; Ghosh, A. A Power Management Scheme for Grid-Connected PV Integrated with Hybrid Energy Storage System. *J. Mod. Power Syst. Clean Energy* **2022**, *10*, 954–963. [CrossRef]
5. Wan, T.; Tao, Y.; Qiu, J.; Lai, S. Data-Driven Hierarchical Optimal Allocation of Battery Energy Storage System. *IEEE Trans. Sustain. Energy* **2021**, *12*, 2097–2109. [CrossRef]
6. Rezvanizaniani, S.M.; Liu, Z.; Chen, Y.; Lee, J. Review and Recent Advances in Battery Health Monitoring and Prognostics Technologies for Electric Vehicle (EV) Safety and Mobility. *J. Power Sources* **2014**, *256*, 110–124. [CrossRef]
7. Wang, J.; Kang, L.; Liu, Y. Optimal Scheduling for Electric Bus Fleets Based on Dynamic Programming Approach by Considering Battery Capacity Fade. *Renew. Sustain. Energy Rev.* **2020**, *130*, 109978. [CrossRef]
8. Zhuang, W.; Lu, S.; Lu, H. Progress in Materials for Lithium-Ion Power Batteries. In Proceedings of the 2014 International Conference on Intelligent Green Building and Smart Grid (IGBSG), Taipei, Taiwan, 23–25 April 2014. [CrossRef]
9. Weiss, H.; Winkler, T.; Ziegerhofer, H. Large Lithium-Ion Battery-Powered Electric Vehicles—From Idea to Reality. In Proceedings of the 2018 ELEKTRO, Mikulov, Czech Republic, 21–23 May 2018; pp. 1–5.
10. Hannan, M.A.; Hoque, M.M.; Hussain, A.; Yusof, Y.; Ker, P.J. State-of-the-Art and Energy Management System of Lithium-Ion Batteries in Electric Vehicle Applications: Issues and Recommendations. *IEEE Access* **2018**, *6*, 19362–19378. [CrossRef]
11. Zubi, G.; Dufo-López, R.; Carvalho, M.; Pasaoglu, G. The Lithium-Ion Battery: State of the Art and Future Perspectives. *Renew. Sustain. Energy Rev.* **2018**, *89*, 292–308. [CrossRef]
12. BYD Blade Battery: Everything You Should Know. Available online: https://topelectricsuv.com/news/byd/byd-blade-battery-update/ (accessed on 1 October 2022).
13. Statista Projected Global Battery Demand from 2020 to 2030, by Application (in Gigawatt Hours). Available online: https://www.statista.com/statistics/ (accessed on 1 October 2022).
14. Plett, G.L. *Battery Management Systems, Volume II: Equivalent-Circuit Methods*; Artech House: Norwood, MA, USA, 2020; Volume II, ISBN 9781630810276.
15. Wang, L.; Qiu, J.; Wang, X.; Chen, L.; Cao, G.; Wang, J.; Zhang, H.; He, X. Insights for Understanding Multiscale Degradation of LiFePO4 Cathodes. *eScience* **2022**, *2*, 125–137. [CrossRef]
16. Meng, J.; Luo, G.; Ricco, M.; Swierczynski, M.; Stroe, D.-I.; Teodorescu, R. Overview of Lithium-Ion Battery Modeling Methods for State-of-Charge Estimation in Electrical Vehicles. *Appl. Sci.* **2018**, *8*, 659. [CrossRef]
17. Feng, X.; Ren, D.; He, X.; Ouyang, M. Mitigating Thermal Runaway of Lithium-Ion Batteries. *Joule* **2020**, *4*, 743–770. [CrossRef]
18. Feng, X.; Ouyang, M.; Liu, X.; Lu, L.; Xia, Y.; He, X. Thermal Runaway Mechanism of Lithium Ion Battery for Electric Vehicles: A Review. *Energy Storage Mater.* **2018**, *10*, 246–267. [CrossRef]
19. Monden, Y.; Mizutani, M.; Yamazaki, S.; Kobayashi, T. Charging and Discharging Control of a Hybrid Battery Energy Storage System Using Different Battery Types in Order to Avoid Degradation. In Proceedings of the 2021 IEEE International Future Energy Electronics Conference (IFEEC), Taipei, Taiwan, 16–19 November 2021; pp. 1–6. [CrossRef]
20. Zhao, Y.; Pohl, O.; Bhatt, A.I.; Collis, G.E.; Mahon, P.J.; Rüther, T.; Hollenkamp, A.F. A Review on Battery Market Trends, Second-Life Reuse, and Recycling. *Sustain. Chem.* **2021**, *2*, 167–205. [CrossRef]
21. Martinez-Laserna, E.; Gandiaga, I.; Sarasketa-Zabala, E.; Badeda, J.; Stroe, D.I.; Swierczynski, M.; Goikoetxea, A. Battery Second Life: Hype, Hope or Reality? A Critical Review of the State of the Art. *Renew. Sustain. Energy Rev.* **2018**, *93*, 701–718. [CrossRef]
22. Dai, H.; Jiang, B.; Hu, X.; Lin, X.; Wei, X.; Pecht, M. Advanced Battery Management Strategies for a Sustainable Energy Future: Multilayer Design Concepts and Research Trends. *Renew. Sustain. Energy Rev.* **2021**, *138*, 110480. [CrossRef]
23. Hossain Lipu, M.S.; Hannan, M.A.; Karim, T.F.; Hussain, A.; Saad, M.H.M.; Ayob, A.; Miah, M.S.; Indra Mahlia, T.M. Intelligent Algorithms and Control Strategies for Battery Management System in Electric Vehicles: Progress, Challenges and Future Outlook. *J. Clean. Prod.* **2021**, *292*, 126044. [CrossRef]
24. Schuster, S.F.; Bach, T.; Fleder, E.; Müller, J.; Brand, M.; Sextl, G.; Jossen, A. Nonlinear Aging Characteristics of Lithium-Ion Cells under Different Operational Conditions. *J. Energy Storage* **2015**, *1*, 44–53. [CrossRef]
25. Deyab, M.A.; Mohsen, Q. Improved Battery Capacity and Cycle Life in Iron-Air Batteries with Ionic Liquid. *Renew. Sustain. Energy Rev.* **2021**, *139*, 110729. [CrossRef]
26. Stroe, D.; Świerczyński, M.; Stan, A.; Teodorescu, R.; Andreasen, S.J. Accelerated Lifetime Testing Methodology for Lifetime Estimation of Lithium-Ion Batteries Used in Augmented Wind Power Plants. *IEEE Trans. Ind. Appl.* **2014**, *50*, 4006–4017. [CrossRef]
27. Meng, J.; Cai, L.; Stroe, D.-I.; Ma, J.; Luo, G.; Teodorescu, R. An Optimized Ensemble Learning Framework for Lithium-Ion Battery State of Health Estimation in Energy Storage System. *Energy* **2020**, *206*, 118140. [CrossRef]
28. Lu, L.; Han, X.; Li, J.; Hua, J.; Ouyang, M. A Review on the Key Issues for Lithium-Ion Battery Management in Electric Vehicles. *J. Power Sources* **2013**, *226*, 272–288. [CrossRef]

29. Xiong, R.; Zhang, Y.; Wang, J.; He, H.; Peng, S.; Pecht, M. Lithium-Ion Battery Health Prognosis Based on a Real Battery Management System Used in Electric Vehicles. *IEEE Trans. Veh. Technol.* **2019**, *68*, 4110–4121. [CrossRef]
30. Farmann, A.; Waag, W.; Marongiu, A.; Sauer, D.U. Critical Review of On-Board Capacity Estimation Techniques for Lithium-Ion Batteries in Electric and Hybrid Electric Vehicles. *J. Power Sources* **2015**, *281*, 114–130. [CrossRef]
31. Cai, L.; Meng, J.; Stroe, D.-I.; Luo, G.; Teodorescu, R. An Evolutionary Framework for Lithium-Ion Battery State of Health Estimation. *J. Power Sources* **2019**, *412*, 615–622. [CrossRef]
32. Sui, X.; He, S.; Vilsen, S.B.; Meng, J.; Teodorescu, R.; Stroe, D.I. A Review of Non-Probabilistic Machine Learning-Based State of Health Estimation Techniques for Lithium-Ion Battery. *Appl. Energy* **2021**, *300*, 117346. [CrossRef]
33. Mohamed, A.T. A Review Paper on Batteries Charging Systems with the State of Charge Determination Techniques. *IET Conf. Publ.* **2019**, *2019*, 1–6. [CrossRef]
34. Qays, M.O.; Buswig, Y.; Hossain, M.L.; Abu-Siada, A. Recent Progress and Future Trends on State of Charge Estimation Methods to Improve Battery-Storage Efficiency: A Review. *CSEE J. Power Energy Syst.* **2019**, *8*, 105–114. [CrossRef]
35. Wang, Y.; Tian, J.; Sun, Z.; Wang, L.; Xu, R.; Li, M.; Chen, Z. A Comprehensive Review of Battery Modeling and State Estimation Approaches for Advanced Battery Management Systems. *Renew. Sustain. Energy Rev.* **2020**, *131*, 110015. [CrossRef]
36. Xiong, R.; Li, L.; Tian, J. Towards a Smarter Battery Management System: A Critical Review on Battery State of Health Monitoring Methods. *J. Power Sources* **2018**, *405*, 18–29. [CrossRef]
37. Xiong, R.; Pan, Y.; Shen, W.; Li, H.; Sun, F. Lithium-Ion Battery Aging Mechanisms and Diagnosis Method for Automotive Applications: Recent Advances and Perspectives. *Renew. Sustain. Energy Rev.* **2020**, *131*, 110048. [CrossRef]
38. Corno, M.; Pozzato, G. Active Adaptive Battery Aging Management for Electric Vehicles. *IEEE Trans. Veh. Technol.* **2020**, *69*, 258–269. [CrossRef]
39. Shi, M.; Shi, X.; Li, Z.; Wang, X. Study on the Aging Characteristics of Li-Ion Battery Based on the Electro-Thermal and Aging Joint Simulation Platform. In Proceedings of the 2020 IEEE/IAS Industrial and Commercial Power System Asia (I&CPS Asia), Weihai, China, 13–15 July 2020; pp. 257–261.
40. Meyer, C.; Bockholt, H.; Haselrieder, W.; Kwade, A. Characterization of the Calendering Process for Compaction of Electrodes for Lithium-Ion Batteries. *J. Mater. Process. Technol.* **2017**, *249*, 172–178. [CrossRef]
41. Schreiner, D.; Klinger, A.; Reinhart, G. Modeling of the Calendering Process for Lithium-Ion Batteries with DEM Simulation. *Procedia CIRP* **2020**, *93*, 149–155. [CrossRef]
42. Mocera, F.; Soma, A.; Clerici, D. Study of Aging Mechanisms in Lithium-Ion Batteries for Working Vehicle Applications. In Proceedings of the 2020 Fifteenth International Conference on Ecological Vehicles and Renewable Energies (EVER), Monte-Carlo, Monaco, 10–12 September 2020. [CrossRef]
43. Stroe, D.I.; Swierczynski, M.; Kær, S.K.; Teodorescu, R. Degradation Behavior of Lithium-Ion Batteries During Calendar Ageing—The Case of the Internal Resistance Increase. *Proc. IEEE Trans. Ind. Appl.* **2018**, *54*, 517–525. [CrossRef]
44. Dufek, E.J.; Tanim, T.R.; Chen, B.-R. Sangwook Kim Battery Calendar Aging and Machine Learning. *Joule* **2022**, *6*, 1363–1367. [CrossRef]
45. Dubarry, M.; Liaw, B.Y.; Chen, M.-S.; Chyan, S.-S.; Han, K.-C.; Sie, W.-T.; Wu, S.-H. Identifying Battery Aging Mechanisms in Large Format Li Ion Cells. *J. Power Sources* **2011**, *196*, 3420–3425. [CrossRef]
46. Mendoza-Hernandez, O.S.; Hosono, E.; Asakura, D.; Matsuda, H.; Shironita, S.; Umeda, M.; Sone, Y. Impact of Calendar Degradation on the Performance of $LiFePO_4$—Graphite Li-Ion Cells during Charge-Discharge Cycling at −5 °C. *J. Electrochem. Soc.* **2019**, *166*, A3525–A3530. [CrossRef]
47. Belt, J.; Utgikar, V.; Bloom, I. Calendar and PHEV Cycle Life Aging of High-Energy, Lithium-Ion Cells Containing Blended Spinel and Layered-Oxide Cathodes. *J. Power Sources* **2011**, *196*, 10213–10221. [CrossRef]
48. Nikitina, V.A. Advanced Electrochemical Analysis of Metal-Ion Battery Materials for Rationalizing and Improving Battery Performance. *Curr. Opin. Electrochem.* **2021**, *29*, 100768. [CrossRef]
49. Guo, J.; Li, Y.; Meng, J.; Pedersen, K.; Gurevich, L.; Stroe, D.-I. Understanding the Mechanism of Capacity Increase during Early Cycling of Commercial NMC/Graphite Lithium-Ion Batteries. *J. Energy Chem.* **2022**, *74*, 34–44. [CrossRef]
50. Fleckenstein, M.; Bohlen, O.; Roscher, M.A.; Bäker, B. Current Density and State of Charge Inhomogeneities in Li-Ion Battery Cells with $LiFePO_4$ as Cathode Material Due to Temperature Gradients. *J. Power Sources* **2011**, *196*, 4769–4778. [CrossRef]
51. Lyu, C.; Zhao, Y.; Luo, W.; Wang, L. Aging Mechanism Analysis and Its Impact on Capacity Loss of Lithium Ion Batteries. In Proceedings of the 2019 14th IEEE Conference on Industrial Electronics and Applications (ICIEA), Xi'an, China, 19–21 June 2019; pp. 2148–2153.
52. Han, X.; Ouyang, M.; Lu, L.; Li, J.; Zheng, Y.; Li, Z. A Comparative Study of Commercial Lithium Ion Battery Cycle Life in Electrical Vehicle: Aging Mechanism Identification. *J. Power Sources* **2014**, *251*, 38–54. [CrossRef]
53. Barré, A.; Deguilhem, B.; Grolleau, S.; Gérard, M.; Suard, F.; Riu, D. A Review on Lithium-Ion Battery Ageing Mechanisms and Estimations for Automotive Applications. *J. Power Sources* **2013**, *241*, 680–689. [CrossRef]
54. Chen, M.; Zhang, L.; Yu, F.; Zhou, L. An Aging Experimental Study of Li-Ion Batteries for Marine Energy Power Station Application. In Proceedings of the 2019 Prognostics and System Health Management Conference (PHM-Qingdao), Qingdao, China, 25–27 October 2019. [CrossRef]
55. Tian, J.; Xiong, R.; Shen, W. State-of-Health Estimation Based on Differential Temperature for Lithium Ion Batteries. *IEEE Trans. Power Electron.* **2020**, *35*, 10363–10373. [CrossRef]

56. Huang, H.; Meng, J.; Wang, Y.; Feng, F.; Cai, L.; Peng, J.; Liu, T. A Comprehensively Optimized Lithium-Ion Battery State-of-Health Estimator Based on Local Coulomb Counting Curve. *Appl. Energy* **2022**, *322*, 119469. [CrossRef]
57. Sataloff, R.T.; Johns, M.M.; Kost, K.M. Fundamentals and Applications of Lithium-Ion Batteries in Electric Drive Vehicles. In *Geriatric Otolaryngology*; Thieme Medical Publishers: New York, NY, USA, 2015; ISBN 9781626239777.
58. *IEC-62660-2*; Secondary Lithium-Ion Cells for the Propulsion of Electric Road Vehicles—Part 2: Reliability and Abuse Testing 2018. International Electrotechnical Commission: Geneva, Switzerland, 2018.
59. *ISO 12405-3*; ISO Electrically Propelled Road Vehicles—Test Specification for Lithium-Ion Traction Battery Packs and Systems—Part 3: Safety Performance Requirements. ISO: Geneva, Switzerland, 2018.
60. *IEEE Std 450-2020 (Revision IEEE Std 450-2010)*; IEEE Recommended Practice for Maintenance, Testing, and Replacement of Vented Lead-Acid Batteries for Stationary Applications. IEEE: New York, NY, USA, 2021; pp. 1–71.
61. Meng, J.; Cai, L.; Stroe, D.-I.; Luo, G.; Sui, X.; Teodorescu, R. Lithium-Ion Battery State-of-Health Estimation in Electric Vehicle Using Optimized Partial Charging Voltage Profiles. *Energy* **2019**, *185*, 1054–1062. [CrossRef]
62. Meng, J.; Cai, L.; Luo, G.; Stroe, D.-I.; Teodorescu, R. Lithium-Ion Battery State of Health Estimation with Short-Term Current Pulse Test and Support Vector Machine. *Microelectron. Reliab.* **2018**, *88–90*, 1216–1220. [CrossRef]
63. Belt, J.R.; Ho, C.D.; Motloch, C.G.; Miller, T.J.; Duong, T.Q. A Capacity and Power Fade Study of Li-Ion Cells during Life Cycle Testing. *J. Power Sources* **2003**, *123*, 241–246. [CrossRef]
64. Wen, A.; Meng, J.; Peng, J.; Cai, L.; Xiao, Q. Online Parameter Identification of the Lithium-Ion Battery with Refined Instrumental Variable Estimation. *Complexity* **2020**, *2020*, 8854618. [CrossRef]
65. Du, X.; Meng, J.; Zhang, Y.; Huang, X.; Wang, S.; Liu, P.; Liu, T. An Information Appraisal Procedure: Endows Reliable Online Parameter Identification to Lithium-Ion Battery Model. *IEEE Trans. Ind. Electron.* **2022**, *69*, 5889–5899. [CrossRef]
66. Xiong, R.; Sun, F.; He, H. Model-Based Health Condition Monitoring Method for Multi-Cell Series-Connected Battery Pack. In Proceedings of the 2016 IEEE Transportation Electrification Conference and Expo (ITEC), Dearborn, MI, USA, 27–29 June 2016; pp. 1–5. [CrossRef]
67. Lin, M.; Wu, D.; Meng, J.; Wu, J.; Wu, H. A Multi-Feature-Based Multi-Model Fusion Method for State of Health Estimation of Lithium-Ion Batteries. *J. Power Sources* **2022**, *518*, 230774. [CrossRef]
68. Tang, X.; Liu, K.; Lu, J.; Liu, B.; Wang, X.; Gao, F. Battery Incremental Capacity Curve Extraction by a Two-Dimensional Luenberger–Gaussian-Moving-Average Filter. *Appl. Energy* **2020**, *280*, 115895. [CrossRef]
69. Maures, M.; Zhang, Y.; Martin, C.; Delétage, J.-Y.; Vinassa, J.-M.; Briat, O. Impact of Temperature on Calendar Ageing of Lithium-Ion Battery Using Incremental Capacity Analysis. *Microelectron. Reliab.* **2019**, *100–101*, 113364. [CrossRef]
70. Feng, X.; Weng, C.; He, X.; Wang, L.; Ren, D.; Lu, L.; Han, X.; Ouyang, M. Incremental Capacity Analysis on Commercial Lithium-Ion Batteries Using Support Vector Regression: A Parametric Study. *Energies* **2018**, *11*, 2323. [CrossRef]
71. Li, L.; Li, Y.; Cui, W.; Chen, Z.; Wang, D.; Zhou, B.; Hong, D. A Novel Health Indicator for Online Health Estimation of Lithium-Ion Batteries Using Partial Incremental Capacity and Dynamic Voltage Warping. *J. Power Sources* **2022**, *545*, 231961. [CrossRef]
72. Tang, X.; Zou, C.; Yao, K.; Chen, G.; Liu, B.; He, Z.; Gao, F. A Fast Estimation Algorithm for Lithium-Ion Battery State of Health. *J. Power Sources* **2018**, *396*, 453–458. [CrossRef]
73. Jiang, Y.; Jiang, J.; Zhang, C.; Zhang, W.; Gao, Y.; Li, N. State of Health Estimation of Second-Life LiFePO4 Batteries for Energy Storage Applications. *J. Clean. Prod.* **2018**, *205*, 754–762. [CrossRef]
74. Li, X.; Wang, Z.; Zhang, L.; Zou, C.; Dorrell, D.D. State-of-Health Estimation for Li-Ion Batteries by Combing the Incremental Capacity Analysis Method with Grey Relational Analysis. *J. Power Sources* **2019**, *410–411*, 106–114. [CrossRef]
75. Ma, H.; Deng, Y.; Liu, W.W.; Li, T.; Zhang, H. State of Health Estimation of Retired Battery for Echelon Utilization Based on Charging Curve. *Procedia CIRP* **2022**, *105*, 458–463. [CrossRef]
76. Li, X.; Jiang, J.; Wang, L.Y.; Chen, D.; Zhang, Y.; Zhang, C. A Capacity Model Based on Charging Process for State of Health Estimation of Lithium Ion Batteries. *Appl. Energy* **2016**, *177*, 537–543. [CrossRef]
77. Bloom, I.; Jansen, A.N.; Abraham, D.P.; Knuth, J.; Jones, S.A.; Battaglia, V.S.; Henriksen, G.L. Differential Voltage Analyses of High-Power, Lithium-Ion Cells: 1. Technique and Application. *J. Power Sources* **2005**, *139*, 295–303. [CrossRef]
78. Han, X.; Feng, X.; Ouyang, M.; Lu, L.; Li, J.; Zheng, Y.; Li, Z. A Comparative Study of Charging Voltage Curve Analysis and State of Health Estimation of Lithium-Ion Batteries in Electric Vehicle. *Automot. Innov.* **2019**, *2*, 263–275. [CrossRef]
79. Honkura, K.; Takahashi, K.; Horiba, T. Capacity-Fading Prediction of Lithium-Ion Batteries Based on Discharge Curves Analysis. *J. Power Sources* **2011**, *196*, 10141–10147. [CrossRef]
80. Han, X.; Ouyang, M.; Lu, L.; Li, J. Cycle Life of Commercial Lithium-Ion Batteries with Lithium Titanium Oxide Anodes in Electric Vehicles. *Energies* **2014**, *7*, 4895–4909. [CrossRef]
81. Liang, T.; Song, L.; Shi, K. On-Board Incremental Capacity/Differential Voltage Curves Acquisition for State of Health Monitoring of Lithium-Ion Batteries. In Proceedings of the 2018 IEEE International Conference on Applied System Invention (ICASI), Tokyo, Japan, 13–17 April 2018; pp. 976–979.
82. Wu, B.; Yufit, V.; Merla, Y.; Martinez-Botas, R.F.; Brandon, N.P.; Offer, G.J. Differential Thermal Voltammetry for Tracking of Degradation in Lithium-Ion Batteries. *J. Power Sources* **2015**, *273*, 495–501. [CrossRef]
83. Zhang, Q.; Wei, F.; Zhang, P.; Dong, R.; Li, J.; Li, P.; Jia, Q.; Liu, Y.; Mao, J.; Shao, G. Research on the Reversible and Irreversible Heat Generation of LiNi1−x−yCoxMnyO$_2$-Based Lithium-Ion Batteries. *Fire Technol.* **2022**. [CrossRef]

84. Maher, K.; Yazami, R. A Study of Lithium Ion Batteries Cycle Aging by Thermodynamics Techniques. *J. Power Sources* **2014**, *247*, 527–533. [CrossRef]
85. Yang, J.; Cai, Y.; Mi, C. Lithium-Ion Battery Capacity Estimation Based on Battery Surface Temperature Change under Constant-Current Charge Scenario. *Energy* **2022**, *241*, 122879. [CrossRef]
86. Birkl, C. *Diagnosis and Prognosis of Degradation in Lithium-Ion Batteries*; University of Oxford: Oxford, UK, 2017.
87. Wang, Z.; Yuan, C.; Li, X. Lithium Battery State-of-Health Estimation via Differential Thermal Voltammetry with Gaussian Process Regression. *IEEE Trans. Transp. Electrif.* **2021**, *7*, 16–25. [CrossRef]
88. Saha, B.; Goebel, K. Battery Data Set. Available online: https://www.nasa.gov/intelligent-systems-division (accessed on 1 October 2022).
89. Wu, Y.; Jossen, A. Entropy-Induced Temperature Variation as a New Indicator for State of Health Estimation of Lithium-Ion Cells. *Electrochim. Acta* **2018**, *276*, 370–376. [CrossRef]
90. Zhang, W.-J. Structure and Performance of LiFePO4 Cathode Materials: A Review. *J. Power Sources* **2011**, *196*, 2962–2970. [CrossRef]
91. Oh, K.-Y.; Epureanu, B.I.; Siegel, J.B.; Stefanopoulou, A.G. Phenomenological Force and Swelling Models for Rechargeable Lithium-Ion Battery Cells. *J. Power Sources* **2016**, *310*, 118–129. [CrossRef]
92. Li, R.; Li, W.; Singh, A.; Ren, D.; Hou, Z.; Ouyang, M. Effect of External Pressure and Internal Stress on Battery Performance and Lifespan. *Energy Storage Mater.* **2022**, *52*, 395–429. [CrossRef]
93. Jeong, J.; Kwak, E.; Kim, J.; Oh, K.-Y. Novel Active Management of Compressive Pressure on a Lithium-Ion Battery Using a Phase Transition Actuator. *Energy Rep.* **2022**, *8*, 10762–10775. [CrossRef]
94. Deich, T.; Hahn, S.L.; Both, S.; Birke, K.P.; Bund, A. Validation of an Actively-Controlled Pneumatic Press to Simulate Automotive Module Stiffness for Mechanically Representative Lithium-Ion Cell Aging. *J. Energy Storage* **2020**, *28*, 101192. [CrossRef]
95. Oh, K.Y.; Siegel, J.B.; Secondo, L.; Kim, S.U.; Samad, N.A.; Qin, J.; Anderson, D.; Garikipati, K.; Knobloch, A.; Epureanu, B.I.; et al. Rate Dependence of Swelling in Lithium-Ion Cells. *J. Power Sources* **2014**, *267*, 197–202. [CrossRef]
96. Samad, N.A.; Kim, Y.; Siegel, J.B.; Stefanopoulou, A.G. Battery Capacity Fading Estimation Using a Force-Based Incremental Capacity Analysis. *J. Electrochem. Soc.* **2016**, *163*, A1584–A1594. [CrossRef]
97. Schiffer, Z.J.; Cannarella, J.; Arnold, C.B. Strain Derivatives for Practical Charge Rate Characterization of Lithium Ion Electrodes. *J. Electrochem. Soc.* **2016**, *163*, A427–A433. [CrossRef]
98. Deng, Z.; Zhang, Z.; Lai, Y.; Liu, J.; Li, J.; Liu, Y. Electrochemical Impedance Spectroscopy Study of a Lithium/Sulfur Battery: Modeling and Analysis of Capacity Fading. *J. Electrochem. Soc.* **2013**, *160*, A553–A558. [CrossRef]
99. Capkova, D.; Knap, V.; Fedorkova, A.S.; Stroe, D.-I. Analysis of 3.4 Ah Lithium-Sulfur Pouch Cells by Electrochemical Impedance Spectroscopy. *J. Energy Chem.* **2022**, *72*, 318–325. [CrossRef]
100. Du, X.; Meng, J.; Peng, J.; Zhang, Y.; Liu, T.; Teodorescu, R. Sensorless Temperature Estimation of Lithium-Ion Battery Based on Broadband Impedance Measurements. *IEEE Trans. Power Electron.* **2022**, *37*, 10101–10105. [CrossRef]
101. Zhang, Y.; Tang, Q.; Zhang, Y.; Wang, J.; Stimming, U.; Lee, A.A. Identifying Degradation Patterns of Lithium Ion Batteries from Impedance Spectroscopy Using Machine Learning. *Nat. Commun.* **2020**, *11*, 1706. [CrossRef]
102. Jiang, B.; Zhu, J.; Wang, X.; Wei, X.; Shang, W.; Dai, H. A Comparative Study of Different Features Extracted from Electrochemical Impedance Spectroscopy in State of Health Estimation for Lithium-Ion Batteries. *Appl. Energy* **2022**, *322*, 119502. [CrossRef]
103. Meddings, N.; Heinrich, M.; Overney, F.; Lee, J.-S.; Ruiz, V.; Napolitano, E.; Seitz, S.; Hinds, G.; Raccichini, R.; Gaberšček, M.; et al. Application of Electrochemical Impedance Spectroscopy to Commercial Li-Ion Cells: A Review. *J. Power Sources* **2020**, *480*, 228742. [CrossRef]
104. Knehr, K.W.; Hodson, T.; Bommier, C.; Davies, G.; Kim, A.; Steingart, D.A. Understanding Full-Cell Evolution and Non-Chemical Electrode Crosstalk of Li-Ion Batteries. *Joule* **2018**, *2*, 1146–1159. [CrossRef]
105. Khan, N.; Ullah, F.U.M.; Afnan; Ullah, A.; Lee, M.Y.; Baik, S.W. Batteries State of Health Estimation via Efficient Neural Networks with Multiple Channel Charging Profiles. *IEEE Access* **2021**, *9*, 7797–7813. [CrossRef]
106. Sihvo, J.; Roinila, T.; Stroe, D.I. SOH Analysis of Li-Ion Battery Based on ECM Parameters and Broadband Impedance Measurements. In Proceedings of the IECON Proceedings (Industrial Electronics Conference), Singapore, 18–21 October 2020; pp. 1923–1928.
107. Wang, X.; Kou, Y.; Wang, B.; Jiang, Z.; Wei, X.; Dai, H. Fast Calculation of Broadband Battery Impedance Spectra Based on S Transform of Step Disturbance and Response. *IEEE Trans. Transp. Electrif.* **2022**, *8*, 3659–3672. [CrossRef]
108. Wang, X.; Wei, X.; Chen, Q.; Dai, H. A Novel System for Measuring Alternating Current Impedance Spectra of Series-Connected Lithium-Ion Batteries with a High-Power Dual Active Bridge Converter and Distributed Sampling Units. *IEEE Trans. Ind. Electron.* **2021**, *68*, 7380–7390. [CrossRef]
109. Huang, W.; Abu Qahouq, J.A. An Online Battery Impedance Measurement Method Using DC–DC Power Converter Control. *IEEE Trans. Ind. Electron.* **2014**, *61*, 5987–5995. [CrossRef]
110. Qahouq, J.A.A.; Xia, Z. Single-Perturbation-Cycle Online Battery Impedance Spectrum Measurement Method with Closed-Loop Control of Power Converter. *IEEE Trans. Ind. Electron.* **2017**, *64*, 7019–7029. [CrossRef]

111. Raijmakers, L.H.J.; Shivakumar, K.M.; Donkers, M.C.F.; Lammers, M.J.G.; Bergveld, H.J. Crosstalk Interferences on Impedance Measurements in Battery Packs**This Work Has Received Financial Support from the Dutch Ministry of Economic Affairs under the Grant A Green Deal in Energy Materials (ADEM) and from the Horizon 2020 Programme of the European Union under the Grant Integrated Components for Complexity Control in Affordable Electrified Cars (3Ccar-662192). *IFAC-PapersOnLine* **2016**, *49*, 42–47. [CrossRef]
112. Wei, X.; Wang, X.; Dai, H. Practical On-Board Measurement of Lithium Ion Battery Impedance Based on Distributed Voltage and Current Sampling. *Energies* **2018**, *11*, 64. [CrossRef]
113. He, C.; Feng, Z. Research on Parmeters of Acquisition Model Based on Non-Linear Least Squares Method. In Proceedings of the 2011 International Conference on Remote Sensing, Environment and Transportation Engineering, Nanjing, China, 24–26 June 2011; pp. 1499–1502. [CrossRef]
114. Toh, K.A.; Eng, H.L. Between Classification-Error Approximation and Weighted Least-Squares Learning. *IEEE Trans. Pattern Anal. Mach. Intell.* **2008**, *30*, 658–669. [CrossRef] [PubMed]
115. Plett, G.L. Recursive Approximate Weighted Total Least Squares Estimation of Battery Cell Total Capacity. *J. Power Sources* **2011**, *196*, 2319–2331. [CrossRef]
116. Kim, E.; Member, S.; Kim, K.; Member, S. Distance Estimation with Weighted Least Squaresfor Mobile Beacon-Based Localization in Wireless Sensor Networks. *Signal Process.* **2010**, *17*, 559–562.
117. Tang, X.; Mao, X.; Lin, J.; Koch, B. Capacity Estimation for Li-Ion Batteries. In Proceedings of the 2011 American Control Conference, San Francisco, CA, USA, 29 June 2011–1 July 2011; pp. 947–952. [CrossRef]
118. Wei, J.; Chen, C. State of Charge and Health Estimation for Lithium-Ion Batteries Using Recursive Least Squares. In Proceedings of the 2020 5th International Conference on Advanced Robotics and Mechatronics (ICARM), Shenzhen, China, 18–21 December 2020; pp. 686–689. [CrossRef]
119. Arablouei, R.; Dogancay, K. Linearly-Constrained Recursive Total Least-Squares Algorithm. *IEEE Signal Process. Lett.* **2012**, *19*, 821–824. [CrossRef]
120. Wei, Z.; Zou, C.; Leng, F.; Soong, B.H.; Tseng, K.J. Online Model Identification and State-of-Charge Estimate for Lithium-Ion Battery with a Recursive Total Least Squares-Based Observer. *IEEE Trans. Ind. Electron.* **2018**, *65*, 1336–1346. [CrossRef]
121. Feng, D.Z.; Bao, Z.; Jiao, L.C. Total Least Mean Squares Algorithm. *IEEE Trans. Signal Process.* **1998**, *46*, 2122–2130. [CrossRef]
122. Rhode, S.; Usevich, K.; Markovsky, I.; Gauterin, F. A Recursive Restricted Total Least-Squares Algorithm. *IEEE Trans. Signal Process.* **2014**, *62*, 5652–5662. [CrossRef]
123. Kim, T.; Wang, Y.; Sahinoglu, Z.; Wada, T.; Hara, S.; Qiao, W. A Rayleigh Quotient-Based Recursive Total-Least-Squares Online Maximum Capacity Estimation for Lithium-Ion Batteries. *IEEE Trans. Energy Convers.* **2015**, *30*, 842–851. [CrossRef]
124. Lai, X.; Zheng, Y.; Sun, T. A Comparative Study of Different Equivalent Circuit Models for Estimating State-of-Charge of Lithium-Ion Batteries. *Electrochim. Acta* **2018**, *259*, 566–577. [CrossRef]
125. Meng, J.; Ricco, M.; Luo, G.; Swierczynski, M.; Stroe, D.I.; Stroe, A.I.; Teodorescu, R. An Overview and Comparison of Online Implementable SOC Estimation Methods for Lithium-Ion Battery. *IEEE Trans. Ind. Appl.* **2018**, *54*, 1583–1591. [CrossRef]
126. Xia, Z.; Abu Qahouq, J.A. Evaluation of Parameter Variations of Equivalent Circuit Model of Lithium-Ion Battery under Different SOH Conditions. In Proceedings of the 2020 IEEE Energy Conversion Congress and Exposition (ECCE), Detroit, MI, USA, 11–15 October 2020; pp. 1519–1523. [CrossRef]
127. Kharisma, M.D.; Ridwan, M.; Ilmiawan, A.F.; Ario Nurman, F.; Rizal, S. Modeling and Simulation of Lithium-Ion Battery Pack Using Modified Battery Cell Model. In Proceedings of the 2019 6th International Conference on Electric Vehicular Technology (ICEVT), Bali, Indonesia, 18–21 November 2019; pp. 25–30. [CrossRef]
128. Plett, G.L. Extended Kalman Filtering for Battery Management Systems of LiPB-Based HEV Battery Packs—Part 3. State and Parameter Estimation. *J. Power Sources* **2004**, *134*, 277–292. [CrossRef]
129. Yu, Q.; Xiong, R.; Yang, R.; Pecht, M.G. Online Capacity Estimation for Lithium-Ion Batteries through Joint Estimation Method. *Appl. Energy* **2019**, *255*, 113817. [CrossRef]
130. Plett, G.L. Extended Kalman Filtering for Battery Management Systems of LiPB-Based HEV Battery Packs—Part 2. Modeling and Identification. *J. Power Sources* **2004**, *134*, 262–276. [CrossRef]
131. Chen, C.; Xiong, R.; Shen, W. A Lithium-Ion Battery-in-the-Loop Approach to Test and Validate Multiscale Dual H Infinity Filters for State-of-Charge and Capacity Estimation. *IEEE Trans. Power Electron.* **2018**, *33*, 332–342. [CrossRef]
132. Wang, H.; Leng, J. A Brief Review on the Development of Kalman Filter. In Proceedings of the 2018 Chinese Control and Decision Conference (CCDC), Shenyang, China, 9–11 June 2018; pp. 694–699. [CrossRef]
133. Xu, L.; Wang, J.; Chen, Q. Kalman Filtering State of Charge Estimation for Battery Management System Based on a Stochastic Fuzzy Neural Network Battery Model. *Energy Convers. Manag.* **2012**, *53*, 33–39. [CrossRef]
134. Rahmoun, A.; Biechl, H.; Rosin, A. SOC Estimation for Li-Ion Batteries Based on Equivalent Circuit Diagrams and the Application of a Kalman Filter. In Proceedings of the 2012 Electric Power Quality and Supply Reliability, Tartu, Estonia, 11–13 June 2012; pp. 273–276. [CrossRef]
135. Yu, Z.; Huai, R.; Xiao, L. State-of-Charge Estimation for Lithium-Ion Batteries Using a Kalman Filter Based on Local Linearization. *Energies* **2015**, *8*, 7854–7873. [CrossRef]

136. Sedighfar, A.; Moniri, M.R. Comparison of Three Well-Known Filters for the Battery State of Health Estimation Application. In Proceedings of the 2018 4th International Conference on Frontiers of Signal Processing (ICFSP), Poitiers, France, 24–27 September 2018; pp. 164–168. [CrossRef]
137. Shen, P.; Ouyang, M.; Lu, L.; Li, J.; Feng, X. The Co-Estimation of State of Charge, State of Health, and State of Function for Lithium-Ion Batteries in Electric Vehicles. *IEEE Trans. Veh. Technol.* **2018**, *67*, 92–103. [CrossRef]
138. Qian, K.F.; Liu, X.T. Hybrid Optimization Strategy for Lithium-Ion Battery's State of Charge/Health Using Joint of Dual Kalman Filter and Modified Sine-Cosine Algorithm. *J. Energy Storage* **2021**, *44*, 103319. [CrossRef]
139. Plett, G.L. Sigma-Point Kalman Filtering for Battery Management Systems of LiPB-Based HEV Battery Packs. Part 1: Introduction and State Estimation. *J. Power Sources* **2006**, *161*, 1356–1368. [CrossRef]
140. Xiong, R.; Mu, H. Accurate State of Charge Estimation for Lithium-Ion Battery Using Dual Uncsented Kalman Filters. In Proceedings of the 2017 Chinese Automation Congress (CAC), Jinan, China, 20–22 October 2017; pp. 5484–5487. [CrossRef]
141. Wang, L.; Wang, L.; Liao, C.; Liu, J. Sigma-Point Kalman Filter Application on Estimating Battery SOC. In Proceedings of the 2009 5th IEEE Vehicle Power and Propulsion Conference, VPPC '09, Dearborn, MI, USA, 7–10 September 2009; pp. 1592–1595. [CrossRef]
142. Sangwan, V.; Kumar, R.; Rathore, A.K. State-of-Charge Estimation for Li-Ion Battery Using Extended Kalman Filter (EKF) and Central Difference Kalman Filter (CDKF). In Proceedings of the 2017 IEEE Industry Applications Society Annual Meeting, Cincinnati, OH, USA, 1–5 October 2017; pp. 1–6. [CrossRef]
143. Ma, L.; Xu, Y.; Zhang, H.; Yang, F.; Wang, X.; Li, C. Co-Estimation of State of Charge and State of Health for Lithium-Ion Batteries Based on Fractional-Order Model with Multi-Innovations Unscented Kalman Filter Method. *J. Energy Storage* **2022**, *52*, 104904. [CrossRef]
144. Liu, F.; Shao, C.; Su, W.; Liu, Y. Online Joint Estimator of Key States for Battery Based on a New Equivalent Circuit Model. *J. Energy Storage* **2022**, *52*, 104780. [CrossRef]
145. Xing, Y.; Ma, E.W.M.; Tsui, K.L.; Pecht, M. A Case Study on Battery Life Prediction Using Particle Filtering. In Proceedings of the IEEE 2012 Prognostics and System Health Management Conference (PHM-2012 Beijing), Beijing, China, 23–25 May 2012. [CrossRef]
146. Cong, X.; Zhang, C.; Jiang, J.; Zhang, W.; Jiang, Y. A Hybrid Method for the Prediction of the Remaining Useful Life of Lithium-Ion Batteries with Accelerated Capacity Degradation. *IEEE Trans. Veh. Technol.* **2020**, *69*, 12775–12785. [CrossRef]
147. Hao, X.; Wu, J. Online State Estimation Using Particles Filters of Lithium-Ion Polymer Battery Packs for Electric Vehicle. In Proceedings of the 2015 IEEE International Conference on Systems, Man, and Cybernetics, Hong Kong, China, 9–12 October 2015; pp. 783–788. [CrossRef]
148. Omariba, Z.B.; Zhang, L.; Sun, D. Remaining useful life prediction of electric vehicle lithium-ion battery based on particle filter method. In Proceedings of the IEEE 3rd International Conference on Big Data Analysis (ICBDA), Shanghai, China, 9–12 March 2018; pp. 412–416. [CrossRef]
149. Cai, L.; Lin, J.; Liao, X. A Data-Driven Method for State of Health Prediction of Lithium-Ion Batteries in a Unified Framework. *J. Energy Storage* **2022**, *51*, 104371. [CrossRef]
150. Liu, X.; Jin, Y.; Zeng, S.; Chen, X.; Feng, Y.; Liu, S.; Liu, H. Online Identification of Power Battery Parameters for Electric Vehicles Using a Decoupling Multiple Forgetting Factors Recursive Least Squares Method. *CSEE J. Power Energy Syst.* **2020**, *6*, 735–742. [CrossRef]
151. Xiong, R.; Sun, F.; Chen, Z.; He, H. A Data-Driven Multi-Scale Extended Kalman Filtering Based Parameter and State Estimation Approach of Lithium-Ion Olymer Battery in Electric Vehicles. *Appl. Energy* **2014**, *113*, 463–476. [CrossRef]
152. Wei, Z.; Zhao, J.; Ji, D.; Tseng, K.J. A Multi-Timescale Estimator for Battery State of Charge and Capacity Dual Estimation Based on an Online Identified Model. *Appl. Energy* **2017**, *204*, 1264–1274. [CrossRef]
153. Zhao, F.; Li, P.; Li, Y.; Li, Y. The Li-Ion Battery State of Charge Prediction of Electric Vehicle Using Deep Neural Network. In Proceedings of the 2019 Chinese Control and Decision Conference (CCDC), Nanchang, China, 3–5 June 2019; pp. 773–777. [CrossRef]
154. Chen, C.-R.; Huang, K.-H. The Estimation of the Capacity of Lead-Acid Storage Battery Using Artificial Neural Networks. In Proceedings of the 2006 IEEE International Conference on Systems, Man and Cybernetics, Taipei, Taiwan, 8–11 October 2006; pp. 1575–1579.
155. Sarvi, M.; Adeli, S. A Neural Network Method for Estimation of Battery Available Capacity. In Proceedings of the 45th International Universities Power Engineering Conference UPEC, Cardiff, UK, 31 August–3 September 2010; pp. 28–32.
156. Zhou, J.; He, Z.; Gao, M.; Liu, Y. Battery State of Health Estimation Using the Generalized Regression Neural Network. In Proceedings of the 2015 8th International Congress on Image and Signal Processing (CISP), Shenyang, China, 14–16 October 2015; pp. 1396–1400. [CrossRef]
157. Zhao, S.; Zhang, C.; Wang, Y. Lithium-Ion Battery Capacity and Remaining Useful Life Prediction Using Board Learning System and Long Short-Term Memory Neural Network. *J. Energy Storage* **2022**, *52*, 104901. [CrossRef]
158. Lei, X.; Chan, C.C.; Liu, K.; Ma, L. Pruning LS-SVM Based Battery Model for Electric Vehicles. In Proceedings of the Third International Conference on Natural Computation (ICNC 2007), Haikou, China, 24–27 August 2007; Volume 3, pp. 333–337.
159. Yan, Q. SOC Prediction of Power Battery Based on SVM. In Proceedings of the 2020 Chinese Control and Decision Conference (CCDC), Hefei, China, 22–24 August 2020; pp. 2425–2429.

160. Zhao, M.; Chen, Y.; Luo, B.; Zhong, L.; Xing, R.L. Research of Battery Capacity Fiber On-Line Intelligent Testing Technology Based on SVM. In Proceedings of the 2008 7th World Congress on Intelligent Control and Automation, Chongqing, China, 25–27 June 2008; pp. 3067–3070. [CrossRef]
161. Chu, L.; Zhou, F.; Guo, J. Investigation of Cycle Life of Li-Ion Power Battery Pack Based on LV-SVM. In Proceedings of the 2011 International Conference on Mechatronic Science, Electric Engineering and Computer (MEC), Jilin, China, 19–22 August 2011; pp. 1602–1605.
162. Xie, J.; Li, W.; Hu, Y. Aviation Lead-Acid Battery State-of-Health Assessment Using PSO-SVM Technique. In Proceedings of the 2014 IEEE 5th International Conference on Software Engineering and Service Science, Beijing, China, 27–29 June 2014; pp. 344–347.
163. He, Z.; Gao, M.; Ma, G.; Liu, Y.; Chen, S. Online State-of-Health Estimation of Lithium-Ion Batteries Using Dynamic Bayesian Networks. *J. Power Sources* **2014**, *267*, 576–583. [CrossRef]
164. Liu, K.; Shang, Y.; Ouyang, Q.; Widanage, W.D. A Data-Driven Approach with Uncertainty Quantification for Predicting Future Capacities and Remaining Useful Life of Lithium-Ion Battery. *IEEE Trans. Ind. Electron.* **2021**, *68*, 3170–3180. [CrossRef]
165. Richardson, R.R.; Birkl, C.R.; Osborne, M.A.; Howey, D.A. Gaussian Process Regression for in Situ Capacity Estimation of Lithium-Ion Batteries. *IEEE Trans. Ind. Informatics* **2019**, *15*, 127–138. [CrossRef]
166. Sun, S.; Sun, J.; Wang, Z.; Zhou, Z.; Cai, W. Prediction of Battery SOH by CNN-BiLSTM Network Fused with Attention Mechanism. *Energies* **2022**, *15*, 4428. [CrossRef]
167. Gu, X.; See, K.W.; Li, P.; Shan, K.; Wang, Y.; Zhao, L.; Lim, K.C.; Zhang, N. A Novel State-of-Health Estimation for the Lithium-Ion Battery Using a Convolutional Neural Network and Transformer Model. *Energy* **2022**, *262*, 125501. [CrossRef]
168. You, G.-W.; Park, S.; Oh, D. Diagnosis of Electric Vehicle Batteries Using Recurrent Neural Networks. *IEEE Trans. Ind. Electron.* **2017**, *64*, 4885–4893. [CrossRef]
169. Raman, M.; Champa, V.; Prema, V. State of Health Estimation of Lithium Ion Batteries Using Recurrent Neural Network and Its Variants. In Proceedings of the 2021 IEEE International Conference on Electronics, Computing and Communication Technologies (CONECCT), Bangalore, India, 9–11 July 2021; pp. 1–6.
170. Zhang, J.; Hou, J.; Zhang, Z. Online State-of-Health Estimation for the Lithium-Ion Battery Based on An LSTM Neural Network with Attention Mechanism. In Proceedings of the 2020 Chinese Control and Decision Conference (CCDC), Hefei, China, 22–24 August 2020; pp. 1334–1339.
171. Ma, Y.; Shan, C.; Gao, J.; Chen, H. A Novel Method for State of Health Estimation of Lithium-Ion Batteries Based on Improved LSTM and Health Indicators Extraction. *Energy* **2022**, *251*, 123973. [CrossRef]
172. Fan, Y.; Xiao, F.; Li, C.; Yang, G.; Tang, X. A Novel Deep Learning Framework for State of Health Estimation of Lithium-Ion Battery. *J. Energy Storage* **2020**, *32*, 101741. [CrossRef]
173. Single Cell Supervisor (Linx) DNB1168 Datang NXP Semiconductors. Available online: https://www.datangnxp.com/en/details/products/43 (accessed on 7 October 2022).